

BERTHIERINE FROM THE LOWER CRETACEOUS CLEARWATER FORMATION, ALBERTA, CANADA

EDWARD R. C. HORNIBROOK AND FREDERICK J. LONGSTAFFE

Department of Earth Sciences, University of Western Ontario, London, Ontario, Canada N6A 5B7

Abstract—Berthierine occurs as pore-linings of well crystallized laths of variable thickness in oil-sands of the Clearwater Formation, Alberta, Canada. Berthierine crystallized early in diagenesis within portions of a deltaic/estuarine complex dominated by brackish to fresh water.

Separates prepared using high gradient magnetic separation contain approximately equal amounts of monoclinic and orthorhombic berthierine. Minor, but variable, quantities of inseparable, iron-rich impurities mainly consist of chamosite Ib and IIb, and Fe-rich smectitic clays.

Clearwater Formation berthierine has a range of chemical compositions that differ from those reported for most other berthierines. The SiO₂ (27–35 wt%), Fe₂O₃ (5–8 wt%) and Al₂O₃ (16–18 wt%) contents for Clearwater Formation berthierine fall between values normally reported for berthierine and odinite. The average structural formula of five samples studied in detail is (Fe²⁺_{1.01}Al_{0.82}Mg_{0.46}Fe³⁺_{0.28}Mn_{<0.01}□_{0.43})(Si_{1.74}Al_{0.26})O₅(OH)₄, where □ represents vacancies in the octahedral sheet. The large number of vacancies in the octahedral sheet implies a di-trioctahedral character for this clay. Our results also suggest that a series of compositions can occur between ideal berthierine and odinite end-members.

Berthierine has been preserved within the Clearwater Formation because temperatures during diagenesis did not exceed 70°C, and perhaps also because hydrocarbon emplacement limited subsequent transformation of berthierine to other phases, such as chamosite. Intense, early diagenetic, microbial activity and/or the strongly reducing environment created by later emplacement of hydrocarbons may be responsible for the Fe²⁺/Fe³⁺ ratio of the berthierine. Because of these conditions, this ratio may have changed since initial clay crystallization. The Clearwater Formation occurrence of grain-coating Fe-rich clays provides valuable insights into possible relationships between the Fe-serpentine minerals, odinite and berthierine, and supports an important role for these phases as precursors to the grain-coating and pore-lining Fe-chlorite (chamosite) that is so common in ancient sandstones, including many hydrocarbon reservoirs.

Key Words—Berthierine, Chamosite, Diagenesis, Neof ormation, Odinite, Oil Sands.

INTRODUCTION

The purpose of this paper is to describe authigenic berthierine from bitumen-saturated sands of the Lower Cretaceous Clearwater Formation, east-central Alberta, Canada. The presence of berthierine in Alberta oil sands has been reported previously (Dean and Nahybida 1985; Prentice and Wightman 1987; Longstaffe et al. 1989a, 1989b, 1992; Longstaffe 1994), but never fully described.

Berthierine is an iron-rich, aluminous, 1:1-type layer silicate belonging to the serpentine group (Brindley 1981). Commonly called septechlorite, septechamosite, chamosite, 7Å-chamosite and/or 7Å-chlorite in the past, berthierine is now the accepted name for this iron-rich, 0.7 nm-layer silicate (Brindley et al. 1968). Berthierine is chemically similar to the iron-rich chlorite, chamosite, with which it also shares a significant number of X-ray powder diffraction (XRD) lines. It is also chemically and structurally similar to the 1:1-layer silicate, odinite, but exhibits several key differences, including the valence state of iron.

Berthierine usually occurs in samples that are mineralogically heterogeneous, making it difficult to study its physical and chemical properties. Frequently, XRD and chemical data for berthierine have been obtained by applying corrections for estimated quantities of

mineral impurities to bulk sample data. The fine-grain size of berthierine also makes single crystal XRD studies unfeasible. Moreover, berthierine commonly contains minute impurities with which it either is intimately associated or, as in the case of chamosite, physically intercalated (Ahn and Peacor 1985; Jiang et al. 1992). As a result, there have been few significant advances in the study of its structure since the early work of Brindley (1949, 1951) and Youell (1955, 1958a).

Berthierine is commonly considered to be typical of marine sediments, probably because of its frequent occurrence in marine-oolitic ironstone formations (e.g. Youell 1958b; Schoen 1964; Bhattacharyya 1983; Van Houten and Purucker 1984; Siehl and Thein 1989). However, non-marine occurrences have been reported, including fresh- to brackish-water sediments of the Early Cretaceous Weald Clay of south-east England (Taylor 1990), a Carboniferous laterite in the USSR (Nikitina and Zvyagin 1972), and a Canadian Arctic desert soil (Kodama and Foscolos 1981). In general though, marine and brackish water occurrences considerably outnumber those known for freshwater. While berthierine most often has been reported as a component of ooids, it also has been described as an authigenic grain-coating or pore-lining in sands (Dean

and Nahnybida 1985; Kantorowicz et al. 1987; Prentice and Wightman 1987; Longstaffe et al. 1989a, 1989b, 1992; Longstaffe 1993).

Other occurrences of berthierine have also been reported. For example, Jiang et al. (1992) described intercalated chlorite-berthierine assemblages of apparent hydrothermal origin where berthierine is thought to have formed as a replacement of chlorite under non-equilibrium, retrograde conditions. This occurrence is of special interest given that berthierine is considered by some to be a diagenetic precursor to chlorite (e.g. Curtis 1990; Longstaffe et al. 1992). Temperatures of 70° to 200°C have been suggested for transformation of berthierine to chamosite during burial diagenesis of such shales and sands, with lower temperatures generally being favored (Velde et al. 1974; Iijima and Matsumoto 1982; Jähren and Aagaard 1989; Walker and Thompson 1990; Longstaffe et al. 1992; Longstaffe 1993). Reports of berthierine intercalated with chlorite are increasing (e.g. Lee and Peacor 1983; Ahn and Peacor 1985; Amouric et al. 1988; Jähren and Aagaard 1989; Hillier and Velde 1992; Jiang et al. 1992), and berthierine may be more common in low temperature environments than generally believed. Admixtures of berthierine with chlorite at very fine scales may easily escape detection during routine mineralogical analysis.

Van Houten and Purucker (1984) summarized possible mechanisms for the origin of berthierine and other "chamositic" minerals, a topic over which there has been some debate. In their discussion, formation by *de novo* growth, or neof ormation, was conceded as a mechanism in circumstances where grain-coatings, pore-linings and void fillings were evident. The general consensus, however, favored early diagenetic, anoxic modification of a precursor accumulated as granules on an oxygenated sea floor. Numerous identities for this early substrate have been proposed (Van Houten and Purucker 1984, and references cited therein).

Recently, the status of green marine clays has been reviewed by Odin (1988) and his coauthors. They suggested that Phyllite V (odinite) could evolve to berthierine during early diagenesis, producing a better organized 0.7 nm structure with only moderate chemical modification. Odinite is a green clay present on many shallow, marine shelves and reef lagoonal areas in tropical locations. It was identified in earlier literature as berthierine (Odin and Giresse 1972; Odin and Matter 1981) or 7Å-chamosite (Porrenga 1965, 1967; Rohrllich et al. 1969). However, Odin (1988) has shown it to be compositionally unique among the layer-silicates and it is now formally recognized as a distinct 0.7 nm phase (Bailey 1988c). Odinite is similar to berthierine in that it is aluminum- and iron-rich, has a 1:1-layer structure and has many of the same XRD lines. However, it is rich in ferric iron, and contains

less Al, and more Mg and Si, than most berthierines currently reported in the literature (Brindley 1982).

Morphological relationships are usually cited as the main difficulty in accepting odinite as a precursor to berthierine (e.g. Humphreys et al. 1989; Van Houten and Purucker 1984). Ancient berthierine is almost exclusively reported as ooids consisting of concentric sheathes around a nucleus of clay, ferric oxide, other ooids, fossil fragments or quartz grains. Reports of well-developed, authigenic grain-coatings or pore-linings are relatively few (Dean and Nahnybida 1985; Kantorowicz et al. 1987; Prentice and Wightman 1987; Longstaffe et al. 1989a, 1989b, 1992; Longstaffe 1993). Similarly, odinite in Recent sediments almost always occurs as peloids of presumed fecal origin. To the best of our knowledge, there are no reports of grain-coating or pore-lining odinite in modern sediments.

The occurrence of pore-lining berthierine in the deltaic sands of the Clearwater Formation provides a special opportunity to explore its origin, in particular berthierine's possible relationships to odinite and chamosite, and the diagenetic conditions that favor its formation and preservation. These sands have experienced only moderate temperatures, and early emplacement of hydrocarbons limited later diagenetic overprinting. The possibility that berthierine might be a precursor to chamosite gives this study further significance. Diagenetic Fe-chlorite commonly occurs as a grain-coating or pore-lining in sandstones. The crystals are distributed in an aggregated, face-to-edge manner that results in significant microporosity and high irreducible water saturations (Longstaffe 1990). The presence of such coatings and linings can limit nucleation of later cements, but also can adversely affect the recoverability of hydrocarbons. Accordingly, how, where and when Fe-rich, diagenetic chlorite, or its precursors, develops within potential reservoir sands can be of substantial, practical importance.

GEOLOGICAL BACKGROUND

The Alberta oil sands are of particular interest because they comprise one of the world's largest accumulations of hydrocarbons. Oil sands stretch from the Athabasca area in the north through the Primrose area to the Cold Lake area in the south (Figure 1), and are contained mostly within the Mannville Group (Figure 2). Bitumen reserves in place are estimated to be about $266 \times 10^9 \text{ m}^3$. The Cold Lake area alone, which is the focus of this paper, contains $35 \times 10^9 \text{ m}^3$ of bitumen in place (Wightman et al. 1989).

The origin of the enormous bitumen reserves in the Alberta oil sands has been debated for a long time. Vigrass (1968) suggested that the bitumen may be related to Lower Cretaceous conventional oils trapped elsewhere in Alberta. Several geochemical investigations have concluded that the Alberta oil sands formed

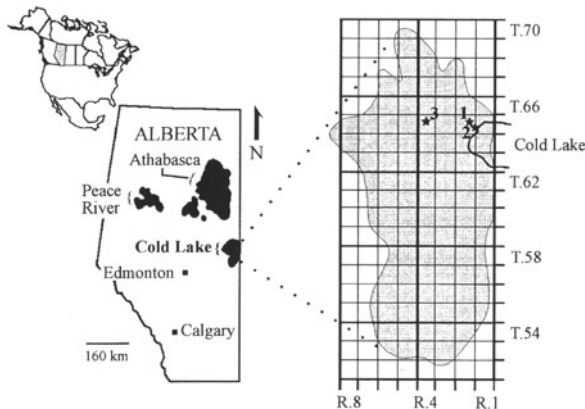


Figure 1. Location of the Cold Lake oil-sand deposit in east-central Alberta (modified from Harrison et al. 1981). Four samples (1-7, 1-16, 2-24 and 2-29) were taken from cores at locations 1 and 2 (both at 8-14-65-2W4; ABC pilot project) and a fifth sample (3-45) was obtained from core at location 3 (3-22-65-4W4; Imperial Oil pilot project).

by biodegradation and water washing of conventional crude oils that had migrated to near-surface traps (Longstaffe 1994, and references therein).

Stratigraphic and Sedimentological Considerations

The Lower Cretaceous Clearwater Formation forms part of the Mannville Group in east-central Alberta (Figure 2). At Cold Lake, the Mannville Group spans depths of about 275 to 600 m, and the regional dip is southwesterly at approximately 1.3 m/km (Wightman et al. 1989). The sediments consist primarily of unconsolidated, siliciclastic materials of both continental and marine origin. They are mostly sands with interbedded siltstones and shales. The sediments lie unconformably on the Paleozoic erosional surface and in turn are overlain conformably by marine shales of the Cretaceous Colorado Group.

In the Cold Lake area, the Mannville Group can be divided into the lowermost McMurray Formation, the overlying Clearwater Formation (including the basal Wabiskaw Member), and the uppermost Grand Rapids Formation, which is commonly split into Lower and Upper Members. Depositional setting is variable, including continental deposits of the McMurray Formation, the marine shelf environment of the Wabiskaw Member, marine shoreline deposits of the Clearwater Formation, and continental to marine shoreline sediments of the Grand Rapids Formation (Wightman et al. 1989). McMurray deposition was dominated by quartzose sediments derived from the Precambrian Shield to the east; volcanic and feldspathic sediments originating mostly from the uplifted western Cordilleran region controlled deposition during Clearwater and Grand Rapids time (Putnam and Pedskalny 1983; Prentice and Wightman 1987).

It is commonly suggested that the berthierine-bearing

Clearwater Formation was deposited as a near-shore, marine, deltaic complex that prograded in a north-northeasterly direction into the boreal seaway, forming a series of overlapping lobes (Harrison et al. 1981; Wightman and Berezniuk 1986). More recently, aspects of estuarine sedimentation have been inferred from the depositional patterns. The deposits themselves are typified by one or more very fine to fine-grained, coarsening upward sequences.

Within the Cold Lake area, the Clearwater Formation has a relatively constant thickness of 35 to 45 m south of Township 64, but thickens to about 65 m in Townships 64 to 66, Ranges 1 to 5W4 (Figure 1) (Wightman and Berezniuk 1986). This latter zone contains the thickest intervals of bitumen-saturated sand (15 to 45 m). Wightman and Berezniuk (1986) suggested that channel switching caused deposition of discrete deltaic lobes. Abandoned lobes became submerged, but not to sufficient depths for substantial deposition of clay prior to growth of the next lobe, thus creating a thick sand at the depo-center. In such a scenario, sands would be expected to thin, and shales become more prominent toward the delta front and margins. The thinning of the Clearwater sands to the north, northeast and northwest of Townships 67-68 (Figure 1) is consistent with such a model (Wightman and Berezniuk 1986).

Using the deltaic model, three sedimentary facies associations have been recognized in typical Clearwater reservoirs: delta-fringe silts and shales, lower delta-front sands and shales, and upper delta-front distributary channels, distributary-mouth bars and beach sands (Harrison et al. 1981; Wightman and Berezniuk 1986; Wightman et al. 1989). The delta fringe consists mainly of silts and shales with minor, thin, discontinuous lenticular sands. Lower delta-front sands are thicker and more continuous, with sand > shale. The upper delta front is composed mostly of relatively thick, uniform sands. The best reservoir sands normally occur in the distributary channel, distributary-mouth bar and beach facies, which are best developed in the south-central portions of the study area.

Sedimentary facies, grain size, fines content and diagenetic clay minerals are the main controls on bitumen saturation and reservoir quality in these sands (Harrison et al. 1981). With decreasing grain size and increasing fines content, bitumen saturation generally decreases. However, for a given grain size or fines content, samples with abundant, grain-coating or pore-lining clays commonly have lower bitumen saturations than samples in which this clay is absent or poorly developed. These clay coatings or linings are abundant in some parts of the distributary channel, distributary-mouth bar and beach sand facies. These units otherwise form the best reservoirs because of their coarser grain sizes and lower fines content relative to other facies. The grain-coating or pore-lining clays original-

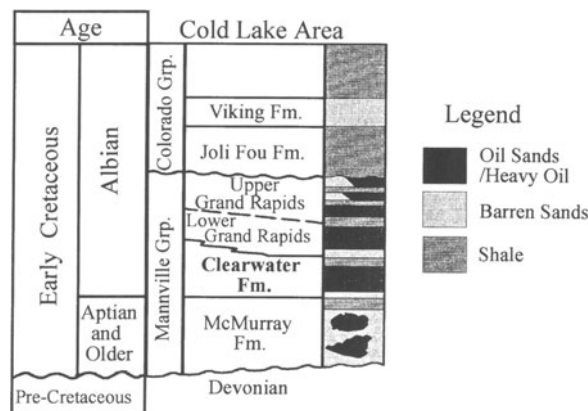


Figure 2. Stratigraphic position of the Clearwater Formation within the Mannville Group in east-central Alberta (after Prentice and Wightman 1987).

ly were identified by Harrison et al. (1981) as Fe-chlorite, but actually are composed mostly of berthierine and related, Fe-rich, clay minerals.

Diagenetic History of the Clearwater Formation

The Clearwater Formation sands are mineralogically immature, consisting mainly of fine or medium-grained, angular or subangular litharenites (classification of Folk 1974; Harrison et al. 1981; Putnam and Pedskalny 1983; Visser et al. 1988; Prentice and Wightman 1987; Hutcheon et al. 1989). Framework-grain mineralogy is dominated by rock fragments, mainly volcanic, chert, metaquartzite and shale fragments, with lesser amounts of plagioclase and monocrystalline quartz; highly altered framework grains are particularly abundant (Prentice and Wightman 1987). Thin calcite \pm siderite-cemented intervals are ubiquitous.

In the Cold Lake area, present burial depths of the Clearwater Formation vary from about 400 to 500 m. Erosion has removed no more than about 1000 m of overlying strata (Hacquebard 1977; Beaumont et al. 1985). Burial history reconstructions suggest that maximum temperatures did not exceed 60–70°C (Longstaffe et al. 1992). Substantial diagenesis has occurred nevertheless because of the very reactive framework mineralogy of these sands. The typical pattern is summarized below, after Longstaffe et al. (1992) and Longstaffe (1993).

Early diagenetic minerals in the bitumen-saturated sands include glauconite, calcite, siderite, pyrite, berthierine and Fe-rich smectitic clays such as interstratified smectite-chlorite, swelling chlorite, and trioctahedral smectitic clays. Alteration and dissolution of framework grains, especially volcanic rock fragments, has been substantial. Localized concretionary carbonate cementation (calcite > siderite) began very early in diagenesis, probably prior to clay diagenesis. These

earlier carbonates most commonly have $\delta^{13}\text{C}_{\text{PDB}}$ values of about 0‰ which is typical of a dominantly inorganic source for carbon, e.g., seawater. Formation of pyrite generally postdated early concretion development, but is relatively uncommon, except immediately below a major sequence boundary within the sands.

Diagenetic berthierine and Fe-rich smectitic clays are confined almost entirely to the thick reservoir sands of the south-central portions of the Cold Lake area, between Townships 65 and 68 (Figure 2). Berthierine is most abundant in sands from distributary-mouth bar and related facies. Within a given package of sediments, it is not uncommon for the abundance of berthierine to decrease (and that of glauconite/illite or smectitic clay to increase) as carbonate concretionary intervals are approached. A slightly later variety of early diagenetic calcite is also abundant in the berthierine-bearing intervals (but is much rarer elsewhere in the Clearwater Formation). This pore-lining or pore-filling calcite is characterized by high $\delta^{13}\text{C}_{\text{PDB}}$ values ($>>0\%$, typical of microbial fermentation). Where relationships can be discerned, this calcite crystallized after berthierine. The iron-poor nature of this calcite (relative to earlier and later varieties) may imply that Fe was preferentially sequestered by early Fe-clay formation, and to a much lesser extent, pyrite. Kaolinite is rare in portions of the deltaic complex that are rich in berthierine and Fe-smectitic clay, but elsewhere, kaolinite is the main diagenetic clay mineral in the bitumen-saturated sands.

K-feldspar and silica overgrowths, along with diagenetic zeolites, siderite and minor euhedral pyrite formed as burial proceeded, together with continued dissolution of volcanic rock fragments and feldspars. Kaolinite continued to form in portions of the deltaic complex (e.g., near its fringes) not dominated by Fe-clays. The latest stage of diagenesis is typified by Fe-rich calcite, generally with $\delta^{13}\text{C}_{\text{PDB}}$ values $<0\%$ (typical of microbial oxidation). Emplacement of hydrocarbons, subsequently altered to bitumen or heavy oil, greatly attenuated subsequent diagenetic mineralization.

Sands from the study area that remained water-saturated, show the same general diagenetic pattern as bitumen-saturated sands with a few notable differences. First, pore-lining clays like berthierine and trioctahedral, Fe-rich smectitic clays are quite rare, whereas kaolinite is common. Second, diagenetic calcite with high $\delta^{13}\text{C}$ values is much less abundant.

ANALYTICAL TECHNIQUES

Samples of oil sands were obtained from three cores previously studied by Longstaffe et al. (1989a, 1989b) (Figure 1). Four samples were taken at locations 1 and 2 (Province of Alberta grid system by legal subdivision, section, township, range and meridian, in that order: 8-14-65-2W4; samples 1-7, 1-16, 2-24 and 2-

Table 1. Sample descriptions.

Sample	Depth	Lithology	Mineralogy of <2 μm size-fraction
1-7	449.75 m	Feldspathic litharenite	Mostly berthierine and dioctahedral ² smectite/illite \pm smectite, with minor calcite, chlorite and illite
1-16	423.10 m	Feldspathic litharenite	Mostly berthierine, with minor calcite, dioctahedral ³ smectite/illite, chlorite and illite
2-24	432.35 m	Feldspathic litharenite	Mostly berthierine, with minor siderite, dioctahedral ³ smectite/illite \pm smectite, chlorite and illite
2-29	443.94 m	Feldspathic litharenite	Mostly berthierine, with minor calcite, siderite, trioctahedral swelling chlorite \pm ³ smectite/chlorite, chlorite and illite
3-45	441.60 m	Feldspathic litharenite	Mostly berthierine, with minor calcite, siderite, pyrite, trioctahedral ⁴ smectite/chlorite \pm smectite, chlorite and illite

¹ All samples saturated by bitumen.

² 80% smectite layers.

³ 60% smectite layers.

⁴ 70% smectite layers.

29; former ABC oil-sand production site). A fifth sample (3-45) was obtained at location 3 (3-22-65-4W4, Imperial Oil oil-sand production site). A brief description of each sample is given in Table 1.

Bitumen was removed from samples by cold extraction using organic solvents, followed by centrifugation and freeze-drying. Samples were then gently sonicated to strip clays that coated grains. The <1 μm size-fraction was then obtained by settling.

Berthierine was separated from the <1 μm clay fraction by liquid High Gradient Magnetic Separation (HGMS) (Tellier et al. 1988). Feed suspension for the separator consisted of the <1 μm size-fraction diluted to a total solids concentration of about 100 mg/litre. Flow velocity was set at about 5 mm/s with a magnetic field of 14.5 kilogauss. The fraction retained by the separator ("mags") was rediluted and reprocessed two more times to obtain a berthierine-enriched separate, as verified by XRD.

SEM examination was performed on bitumen-extracted sands, mounted on aluminum stubs that had been smeared with carbon paste, using an ISI DS-130 scanning electron microscope equipped with a LINK energy dispersive spectrometer.

Powder XRD analysis was performed using a Rigaku rotating anode diffractometer equipped with a graphite monochromator, and CoK α radiation pro-

duced by a current of 45 mA and a potential of 160 kV. Randomly oriented mounts were scanned from 2 to 82° two theta at a rate of 10°/minute. Mounts with a preferred orientation were scanned at the same rate but from 2 to 42° two theta. Samples were prepared as oriented mounts on glass slides and dried overnight at 60°C prior to glycolation. The slides were saturated with ethylene glycol in an evacuated dessicator for 6 hours.

Stepwise heatings of the clay separate were performed both in air and under vacuum. In the first instance, 20 mg of sample was placed in a porcelain crucible and heated for 2 h at temperatures of 300°C, 550°C, 650°C and 900°C, following Brindley and Youell (1953). After each heating, a randomly oriented mount was examined by XRD. In the second instance, 20 mg of sample was placed into a 1.5 cm diameter quartz glass tube attached to a high vacuum line and heated *in situ* for 2 h at temperatures ranging from 50 to 700°C in 50° increments. To limit atmospheric oxidation, the sample was cooled to room temperature under vacuum prior to XRD examination of randomly oriented mounts.

Infrared spectroscopy was performed using a Nicolet 205 Fourier transform infrared spectrometer (FTIR). Samples were prepared as KBr disks using standard methods. Each spectrum consisted of 32 scans at a resolution of 4 cm^{-1} .

Samples were prepared for electron microprobe analysis by pressing about 20 mg of berthierine into pellets at a pressure of 5 tons. The pellets were glued to brass mounts and coated with carbon. Chemical analyses were obtained using a JEOL JXA-8600 electron microprobe equipped with a backscatter electron detector and a Tracor-Northern 5500 automation and energy dispersive system. A 5 μm beam was used with a 20 second counting period.

Chemical analyses by inductively coupled plasma atomic emission spectroscopy (ICP-AES) were performed at the University of Ottawa using the standard lithium borate fusion technique. Structural and adsorbed water analyses were performed by XRAL Laboratories (Don Mills, Ontario) using standard methods.

Mössbauer spectroscopy was performed at the University of Alberta. ⁵⁷Fe Mössbauer spectra were acquired at 298°K with a 50-mCi Co/Rh source on powdered samples that were sandwiched between two layers of scotch tape. The amount of absorber was adjusted to yield absorber thickness of about 5 mg Fe/cm² to avoid saturation effects (Bancroft 1973). The samples were mixed with powdered sucrose to minimize orientation effects. The mirror-image Mössbauer spectra were recorded on 512 channels of a microcomputer-based multichannel analyzer. A velocity range of about 4 mm/s was used and samples were counted until about 10⁶ counts/channel were obtained. The velocity was calibrated with an Fe foil that had values

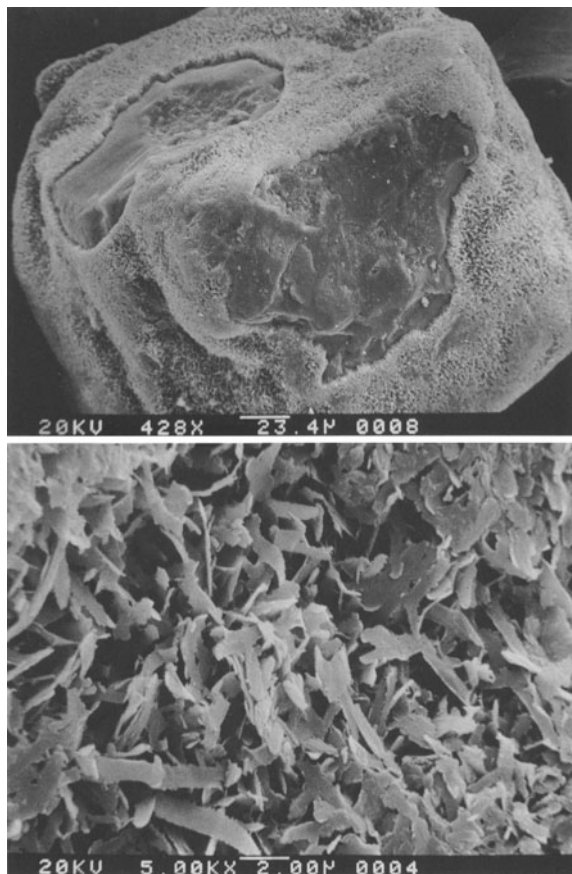


Figure 3. (A) Berthierine coating a feldspar grain. Barren patches are previous contact points with other grains; pressure solution pits are apparent at the contact points. (B) Well-developed networks of berthierine laths.

of $g_0=3.9156$ and $g_1=2.2363$ mm/s (Stevens IG and Stevens VE 1972). The full widths at half maximum were 0.23 mm/s and 0.24 mm/s for the inner and outer lines of the spectra of the Fe foil, respectively. The isomer shifts are reported relative to Fe metal.

Oxygen- and hydrogen-isotope results are reported in the usual δ -notation relative to Vienna Standard Mean Ocean Water (V-SMOW). Oxygen was extracted from the clay minerals using the BrF_5 method of Clayton and Mayeda (1963) and quantitatively converted to CO_2 over red-hot graphite. Samples were preheated at 150°C prior to treatment with BrF_5 . Silica standard NBS-28 gave an average measured $\delta^{18}\text{O}$ value of $9.7 \pm 0.2\text{‰}$. Reproducibility was better than $\pm 0.3\text{‰}$ for all samples. Most hydrogen-isotope measurements on berthierine were performed using the uranium technique and heating methods described by Bigeleisen et al. (1952) and as modified by Kyser and O'Neil (1984). The method of Vennemann and O'Neil (1993) based on zinc reagent and heating with a torch, was used for two samples (but with depleted uranium rath-

er than zinc), producing virtually identical results (-119‰) to the more conventional method (-122 to -117‰ ; average 119‰). Reproducibility was better than $\pm 0.5\text{‰}$. Laboratory standards calibrated to V-SMOW and SLAP were accurate to $\pm 2\text{‰}$. Results obtained for NBS-30 biotite (-66.0‰) and SURRC chlorite (-41.3‰) compare well with internationally accepted values. $^{18}\text{O}/^{16}\text{O}$ and D/H ratios were measured, respectively, on a VG Optima and a VG Prism Series II mass spectrometer.

RESULTS AND DISCUSSION

Mode of Occurrence

Clearwater Formation berthierine occurs as pore-linings of variable thickness that can almost entirely envelop framework grains (Figure 3a). Barren patches visible on some grain edges represent contact points with other grains. The centers of some barren patches exhibit pressure solution pits. The berthierine is most common as well developed networks of laths that have individual dimensions of approximately $\leq 6\mu\text{m} \times \leq 1\mu\text{m} \times \leq 0.1\mu\text{m}$ (Figure 3b). However, in samples of lower crystallinity, and/or as admixture with Fe-rich smectitic clays increases, the clay assemblage becomes more crenulated, and well defined laths are less obvious.

Berthierine Separation

Figure 4 shows oriented XRD traces for two representative samples at different stages of separation. Traces A (sample 2-29) and D (sample 3-45) represent material retained in suspension after sonication in distilled water to strip diagenetic clays from grains. At this stage, the samples primarily consist of quartz, feldspar and a mixture of 0.7, 1.0 and 1.4 nm phyllosilicates. Traces B (sample 2-29) and E (sample 3-45) represent the $<1\mu\text{m}$ material obtained by settling. They show a significant reduction in the relative abundance of quartz, feldspar and 1.0 nm clays. Scans C (sample 2-29) and F (sample 3-45) represent the magnetic fraction of the $<1\mu\text{m}$ material after three passes through the HGMS separator. The majority of final separates show only a minor 1.4 nm diffraction, but a few still contain a trace of 1.0 nm material (e.g., Figure 4f).

Glycolation

Glycolation of the magnetically-enriched fraction resulted in a shift of part of the 1.4 nm diffraction to 1.7 nm (Figure 5). Sample 2-24 contains only a minor amount of the 1.4 nm phase. Glycolation caused a shift of the small and poorly defined 1.4 nm diffraction to higher d-spacings, but did not result in any significant improvement of peak shape (Figure 5, traces A and B). By comparison, sample 3-45 contains a higher abundance (Figure 5, traces C and D) of apparent 1.4 nm mineral. Upon glycolation, a 1.7 nm peak appears.

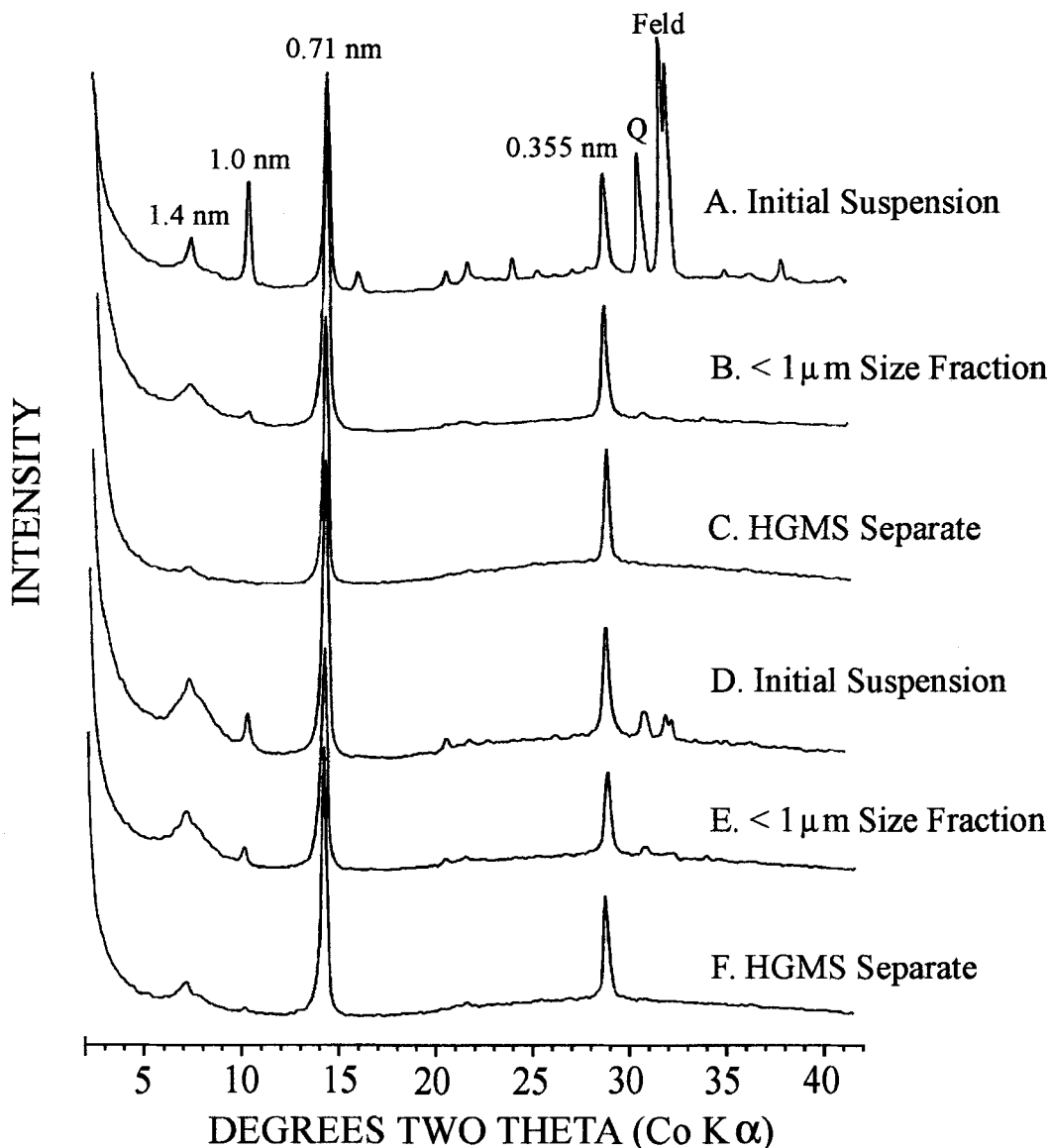


Figure 4. Oriented XRD traces (air dried) for Clearwater samples 2-29 (A-C) and 3-45 (D-F) at different stages of separation. A & D, sonicated suspension; B & E, <1 μm size fraction; and, C & F, magnetic fraction after liquid high gradient magnetic separation (three passes).

Polytypism

XRD traces of randomly oriented samples (Figure 6) suggest that the HGMS-enriched samples contain a mixture of monoclinic (B_m) and orthohexagonal (B_o) forms of berthierine (JCPDF Card Nos. 7-315 (B_m) and 31-618 (B_o)) and possibly, the Ib and Iib polytypes of chamosite (JCPDF Card Nos. 13-29 (Ib); 7-166 and 21-1227 (Iib)). There are many overlapping diffractions between the two sets of polytypes. Monoclinic berthierine has the greatest overlap with the chamosite Iib polytype (monoclinic) and orthohexagonal berthierine with chamosite Ib (orthorhombic). When a

diffraction is common to both forms of berthierine, it is also shared by the two chamosite polytypes, with only a few exceptions.

Preliminary HRTEM studies confirm the presence of a Fe-rich 0.7 nm clay in these Clearwater sands (Longstaffe and Tazaki unpublished data; Zhou, pers. comm. 1995). Some interstratification with 1.4 nm clay also has been observed, but in general 0.7 nm clay is dominant. These observations support the XRD results, which alone can not provide irrefutable evidence that berthierine, as opposed to chamosite, is the sole or dominant Fe-rich clay present in the separates.

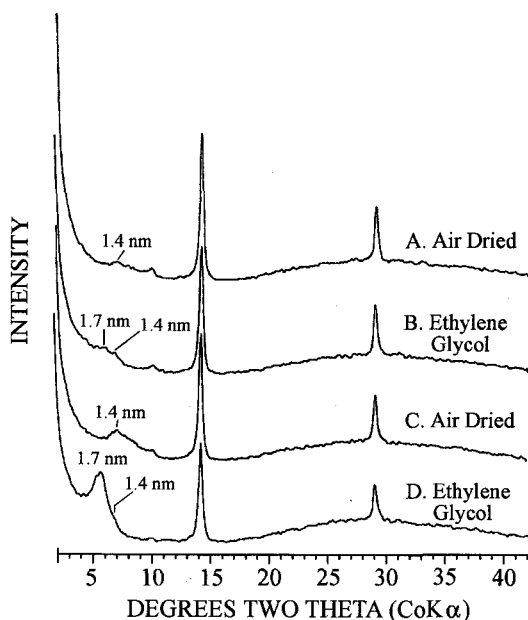


Figure 5. Oriented XRD traces for Clearwater samples 2-24 (A & B) and 3-45 (C & D), before and after treatment with ethylene glycol.

Several areas in the XRD pattern exist that provide further insight into the clay mixture. In particular, among the iron-rich phyllosilicates, a 0.428 nm diffraction (Figure 6, Area 1) appears to be unique to monoclinic berthierine and supports the existence of at least one discrete polytype of berthierine in Clearwater sands, since chamosite polytypes normally do not possess a 0.458 nm diffraction. However, a range of similar d-spacings (0.457 to 0.463 nm) do occur in ferroan clinocllore and saponite.

Diffractions unique to chamosite IIb should be located in the intervals between the three sharp peaks in Area 2 of Figure 6. No well-formed maxima are observed, only a notable increase in background intensity. In this region, the peak/baseline intensity ratio decreases as the intensity of the 1.4 nm diffraction increases (e.g., Figure 6, trace B). Chamosite IIb also possesses several low intensity diffractions between peaks 0.178 and 0.168 nm. The broad and poorly formed character of diffractions attributable solely to chamosite IIb suggest that it has a poorly crystalline structure and is limited in abundance. By comparison, the sharpness and intensity of the majority of peaks in the pattern indicate the dominant phase(s) to be well-ordered. The similarity in shape of isolated monoclinic

berthierine maxima (e.g., 0.428 nm) to most other diffractions in the rest of the pattern suggest that berthierine may constitute the bulk of well-crystalline material.

A number of diffractions (e.g., 0.252, 0.215, 0.178, 0.1481 nm) confirm the existence of a second polytype in Clearwater samples. Based on the intensity and similarity of peak shape to co-existing monoclinic berthierine, this second form is most likely orthohexagonal berthierine. However, chamosite Ib cannot be distinguished here on the basis of isolated, unique diffractions (with the exception of the 1.4 nm maxima), hence the presence of discrete well-crystallized chamosite Ib cannot be completely ruled out. However, it is more probable that a mixture of well-ordered monoclinic and orthohexagonal berthierine coexists with both (poorly-ordered) chamosite polytypes. In addition, glycolation of the samples has shown that typically minor, but variable, quantities of Fe-rich smectitic clays are also present, similar to those previously described by Dean and Nahnybida (1985) and Longstaffe et al. (1989a) (e.g., interstratified smectite-chlorite, swelling chlorite, trioctahedral smectitic clays). The presence of even minimal quantities of these clays in the HGMS separates further complicates unique recognition of chlorite given their similar (001) basal diffractions in air-dried samples (≈ 1.4 nm). We suggest that, in the Clearwater Formation, well-crystallized berthierine has persisted because of the rather unique, bitumen-saturated, low temperature ($<70^\circ\text{C}$) diagenetic environment. The chamosite (and perhaps Fe-rich smectitic clays?) detected may represent early and incomplete stages of transformation from berthierine.

The presence of other Fe-rich clays also makes it difficult to estimate the proportions of monoclinic and orthohexagonal berthierine. If it is assumed that the contaminants primarily cause an increase in background intensity and a broadening of peaks proportional to the intensity of the 1.4 nm diffraction, then the two forms of berthierine occur in roughly equal amounts based on the data of Brindley (1951). The proportion of the two polytypes appears to remain constant with depth in each bore hole and to vary only slightly between different localities. According to Bailey (1988a), distinctive patterns of metastable 1:1 structures transforming to more stable 1:1 structures with increasing depth of burial are not common. Instead the 1:1 structures, regardless of polytype, are more likely to attain a different structural arrangement (i.e., 2:1, 2:2) as temperature increases. While Bailey

→

Figure 6. XRD traces (randomly oriented samples, air dried) for Clearwater samples 2-29 (A) and 3-45 (B). Key: Fe-smect = Fe-smectitic clays; cham = Fe-chlorite (chamosite); B_m = monoclinic berthierine; B_o = orthohexagonal berthierine; C_{1b} = chamosite Ib polytype (orthorhombic); C_{11b} = chamosite IIb polytype (monoclinic); Q = quartz.

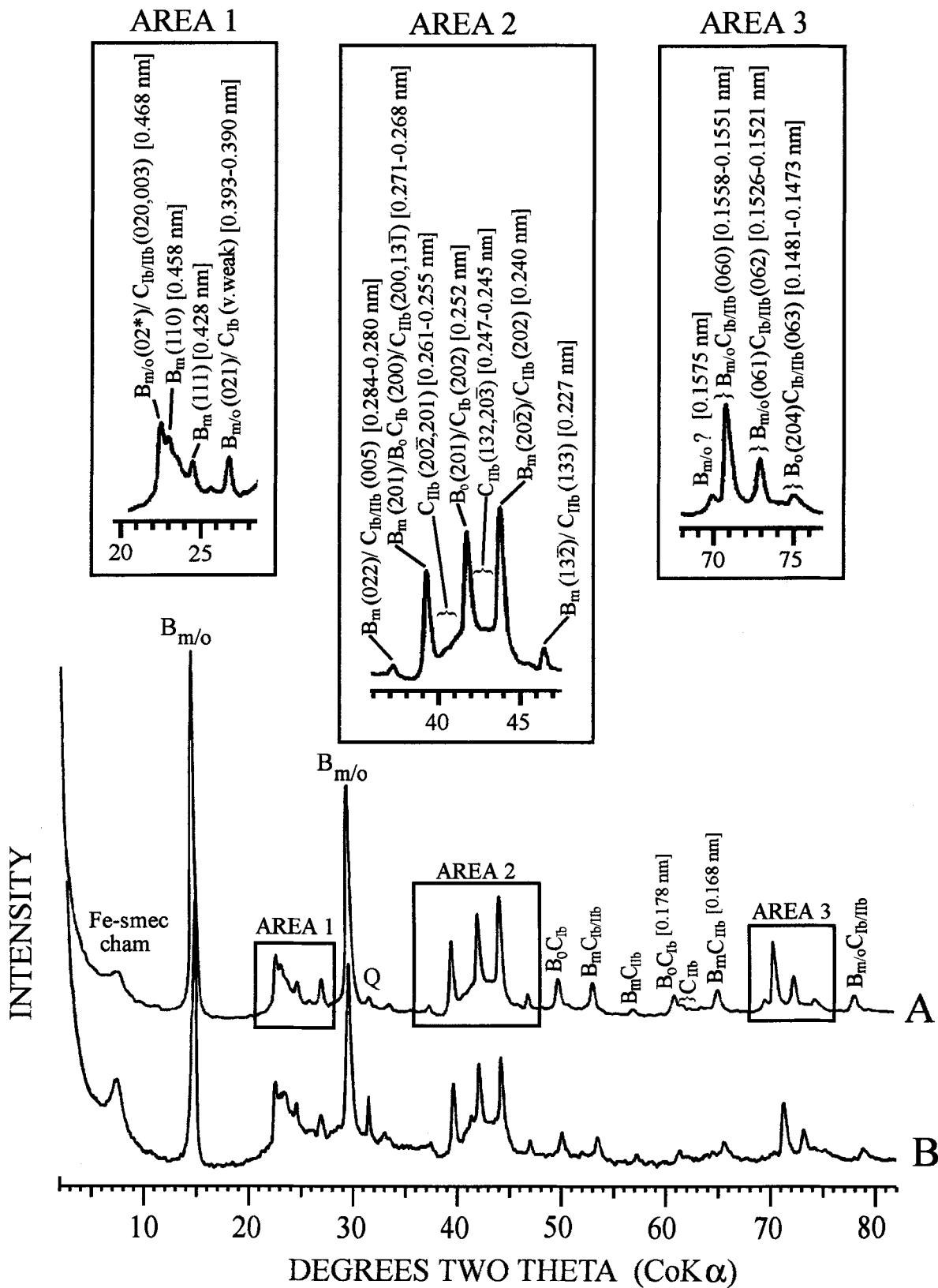


Table 2. Major¹ and trace² element chemistry, and structural formulae for Clearwater berthierine.

	1-7 ³	1-16 ³	2-24 ⁴	2-29 ⁴	3-45 ⁴
SiO ₂	35.76	30.12	33.03	27.32	31.05
Al ₂ O ₃	17.20	16.80	16.01	16.46	15.96
Fe ₂ O ₃	6.69	6.56	7.52	7.89	5.18
FeO	21.48	25.82	21.31	21.42	18.76
MgO	5.57	5.54	5.29	5.21	5.86
MnO	0.10	0.06	0.07	0.06	0.05
TiO ₂	1.96	0.24	0.83	0.76	1.18
K ₂ O	0.75	0.37	1.03	0.65	0.31
Na ₂ O	0.13	0.13	0.23	0.18	0.47
CaO	0.40	0.42	0.81	0.70	0.82
H ₂ O ⁺	9.30	11.90	11.70	11.20	14.30
H ₂ O ⁻	2.30	1.50	1.50	1.70	1.90
Total ⁵	101.64	99.46	99.33	93.55	95.84
Cr	—	—	279	307	330
Cu	—	—	288	384	246
Ni	—	—	142	56	49
V	—	—	573	598	531
Zn	—	—	452	503	449
Si	1.843	1.657	1.798	1.616	1.802
Al(IV)	0.157	0.343	0.202	0.384	0.198
Al(VI)	0.888	0.746	0.825	0.763	0.893
Fe ³⁺	0.259	0.272	0.308	0.351	0.226
Fe ²⁺	0.926	1.188	0.970	1.059	0.910
Mg	0.428	0.454	0.429	0.459	0.507
Mn	0.004	0.003	0.003	0.003	0.002
□	0.495	0.337	0.465	0.365	0.461
O	5.402	5.000	5.000	5.000	5.000
OH	3.197	4.000	4.000	4.000	4.000
H ₂ O	—	0.367	0.248	0.418	1.535
R ³⁺ oct	1.147	1.018	1.133	1.114	1.120
Al tetr	0.157	0.343	0.202	0.384	0.198

¹ Major elements in weight per cent oxides.

² Trace elements expressed in parts per million. Analyzed by ICP-AES with accuracy and precision both better than $\pm 3\%$ based on duplicates and standards.

³ Analysis by electron microprobe only. Precision and accuracy for major elements (Si, Fe, Al, Mg) was better than $\pm 2\%$; minor elements (Mn, Mg, K, Na, Ti) had similar accuracy based on standards, but precision was poorer ($\approx \pm 5\%$).

⁴ Analyses are an average of ICP-AES and electron microprobe measurements. Major oxides by the two methods differed by less than 2 wt%. In general, results between the two methods differed by less than $\pm 5\%$.

⁵ Samples with low totals have had SiO₂ subtracted to correct for quartz impurities.

(1988a) shows that compositional preferences exist for specific metastable 1:1 layer stacking sequences, the typical range of chemistries tolerated by a single polytype are greater than those exhibited in all samples of Clearwater berthierine.

Clearwater berthierine has cell dimensions of $a = 0.5352$ nm, $b = 0.9342$ nm, and $c = 0.7116$ nm based on the (200), (060) and (002) diffractions. Each of these peaks is common to both monoclinic and orthorhombic polytypes, and hence only a generalized set of cell parameters can be provided. The b and c dimensions are at the low end of those reported by Brindley (1951) and Brindley and Youell (1953) for the

two polytypes (1M, $b = 0.933$ nm, $c = 0.728$ nm; 1H, $b = 0.9379$ nm, $c = 0.7114$ nm). The a dimension is well below the value given for either polytype (1M, $a = 0.541$ nm; 1H, $a = 0.5415$ nm). One possible explanation is the higher ferric/ferrous ratio in Clearwater berthierine (Table 2) compared to most reported in the literature (cf. Brindley 1982). Octahedral Fe³⁺ results in a significant contraction of the a and b parameters, since it influences the entire structure in the ab plane (Brindley and Youell 1953). The effect is less dramatic in the [001] direction since it only affects $\frac{1}{3}$ of the structure. Also, a large 2-dimensional diffraction band at 0.468 nm (i.e., $k \neq 3n$) (Figure 6, Area 1) suggests that imperfections exist in the form of $\pm b/3$ layer shifts in Clearwater berthierine (Brindley 1961).

In most layer silicates, tetrahedral sheet dimensions are larger than those of the octahedral sheet and only minor structural adjustments are required to achieve a fit between them (Bailey 1980). More drastic changes, resulting in peculiar morphologies (e.g., curling of 1:1 layers), are required when a - b dimensions of the tetrahedral sheet are smaller than those of the octahedral sheet. This is normally the case for serpentine minerals. However, the unique morphology of Clearwater Formation berthierine (laths) may indicate a much closer fit between the octahedral and tetrahedral sheets. The chemistry (see below) of this berthierine, substitution of Al atoms for Si in the tetrahedral sheet, coupled with trivalent substitutions (Al and Fe³⁺) in the Fe²⁺-dominated octahedral sheet, is consistent with such an observation.

Heating in Air

A portion of sample 2-24 containing a greater quantity of impurities was selected for stepwise heating in air because changes in the intensity of the 1.4 nm peak also were of interest, and a greater abundance of quartz was useful as an internal calibrant for measuring changes in d-spacings. XRD patterns following each heat treatment are shown in Figure 7. Trace A shows the initial mixture of monoclinic and orthorhombic berthierine with admixtures of quartz and poorly crystalline 1.4 nm phase(s). Heating to 300°C causes significant breakdown of the berthierine structure with transformation to a mixed dioctahedral-trioctahedral state. However, the (001) and (002) diffractions have not begun to contract, suggesting that the majority of changes are occurring in the ab dimension. The 1.4 nm peak has undergone a significant reduction in intensity.

Brindley and Youell (1953) and Mackenzie and Berzowski (1984) also produced a range of mixed valence states during heating (in air) of berthierine to 400°C. Similar to those studies, the initial monoclinic and orthorhombic forms of Clearwater berthierine were oxidized to a single orthorhombic, dominantly ferric form. However, the d-values in trace B (0.2482,

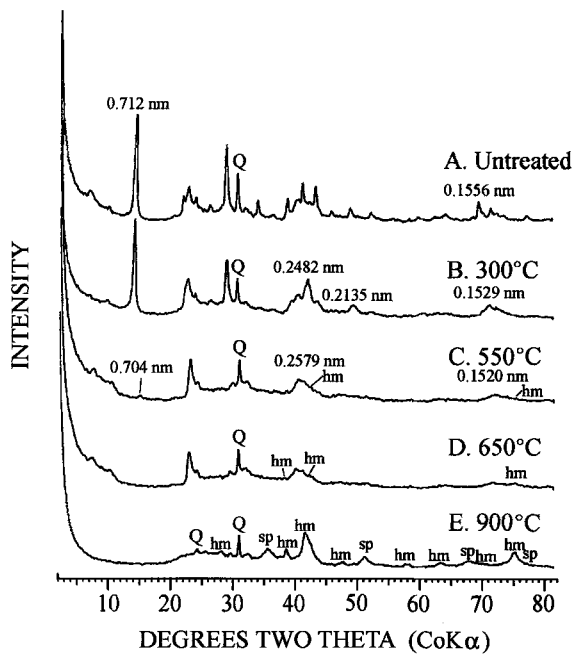


Figure 7. XRD traces (randomly oriented samples) for Clearwater sample FL1-7 during stepwise heating in air. Key: Q = quartz; hm = hematite; sp = spinel group mineral.

0.2135, 0.1529 nm) are slightly higher than those reported by Brindley and Youell (1953) (0.2460, 0.2103, 0.1514 nm) for pure, ferric, orthohexagonal berthierine; a portion of the octahedral iron probably has remained in the ferrous state in the Clearwater berthierine.

At 550°C, only residual (001) and (002) berthierine diffractions remain at 0.7035 and 0.3516 nm, respectively. Other berthierine diffractions have coalesced and shifted to large, broad maxima at 0.4501, 0.2579 and 0.1520 nm, similar to the changes observed by Kodama and Foscolos (1981) and Taylor (1990). The increase in intensity of the 1.4 nm diffraction to the untreated level indicates that dehydroxylation of chlorite has occurred. A small quantity of synthetic hematite has begun to form.

The berthierine structure is completely destroyed at 650°C; however, the major, broad diffractions observed at 550°C remain, but with decreased intensities. The 1.4 nm phase persists, and production of synthetic hematite has increased slightly. At 900°C, all phyllosilicates have been destroyed, synthetic hematite is the most abundant crystalline phase, and quartz persists. Other studies (e.g., Brindley and Youell 1953; Kodama and Foscolos 1981; Taylor 1990) have reported at least a partial transformation of quartz to cristobalite by 900°C. Our only evidence for the latter mineral is a minor diffraction at ~ 0.402 nm, corresponding to the major diffraction of synthetic cristobalite. A spinel group mineral has begun to form, but is too poorly

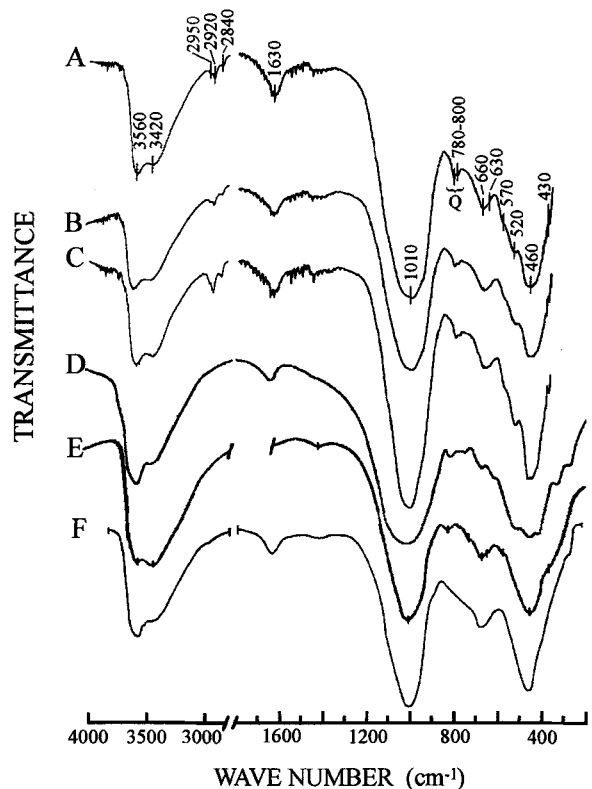


Figure 8. Infrared spectra for berthierine from: A-C = Clearwater Formation; D = Arctic desert soil (Kodama and Foscolos 1981); and E = Kongeus Mine, Kongsberg, Norway (Mackenzie and Berezowski 1984). Spectrum F is for odinite (from Bailey 1988c).

crystalline to be positively identified by XRD as either true spinel (MgAl_2O_4) or hercynite (FeAl_2O_4), although the latter is most likely in this system.

Infrared Spectrometry

Typical infrared spectra of Clearwater berthierines are shown in Figure 8 (A, B, and C). They closely resemble spectra reported for berthierine from an Arctic desert soil (Figure 8D) (Kodama and Foscolos 1981) and the Kongeus Mine, Kongsberg, Norway (Figure 8E) (Mackenzie and Berezowski 1984). The five berthierine spectra also are remarkably similar to one reported by Bailey (1988c) for odinite (Figure 8F).

Assignment of spectral bands was made by analogy with related iron-containing layer silicates, similar to the method of Mackenzie and Berezowski (1984). Two peaks are resolved in the hydroxyl stretching region ($3400\text{--}3600\text{ cm}^{-1}$) at 3560 and 3420 cm^{-1} . The width of these bands suggest a complex, possibly disordered structure with inhomogeneity of octahedral site occupancy (Farmer 1974). Mackenzie and Berezowski (1984) attribute the two vibrations to hydroxyl group bonding with Al-O and Si-O, and note the possibility of random substitution of Al for Si in the tetrahedral

sheet, similar to that reported in amesite by Serna et al. (1977). The vibration at 3420 cm^{-1} has also been attributed to adsorbed water (stretching mode), in addition to a water bending mode band at 1630 cm^{-1} (Bailey 1988c). Major Si-O vibrations occur at 1010 cm^{-1} (stretching mode with a complementary shoulder at 990 cm^{-1}) and at $450\text{--}460\text{ cm}^{-1}$ (bending mode). An additional Si-O vibration occurs at 660 cm^{-1} ; however, its position will vary (660 to 680 cm^{-1}) depending on the quantity of octahedral Fe^{3+} (shifts to lower frequencies occurring as a result of higher concentrations) (Mackenzie and Berezowski 1984). The range of vibrations occurring from 520 to 630 cm^{-1} are attributed to $\text{M}^{3+}\text{-O-Si}$ vibrations, Al^{3+} and Fe^{3+} at the higher and lower frequencies, respectively. A poorly resolved band at 430 cm^{-1} corresponds to $\text{Fe}^{2+}\text{-O-Si}$ vibrations (Mackenzie and Berezowski 1984). A small quantity of quartz impurity is confirmed by the presence of bands at $780\text{--}800\text{ cm}^{-1}$.

Chemical Composition and Structural Formulae

Table 2 lists chemical analyses and structural formulae obtained for the five berthierine samples. The data have been corrected (i.e., excess SiO_2 subtracted) for quartz impurities based on XRD analysis of quartz-doped samples. Results for samples 2-24, 2-29 and 3-45 are an average of electron microprobe (3 analyses each) and ICP-AES (1 analysis each, except for 2-24 which was measured in duplicate) measurements. Values for specimens 1-7 and 1-16 are an average of three microprobe analyses only. Trace element chemistry for samples 2-24, 2-29 and 3-45 were obtained by ICP-AES. No corrections were made for the traces of 1.4 nm clay impurities since their abundance could not be accurately estimated. However, enriched separates of the 1.4 nm phase from Clearwater sands have chemical compositions very similar to those of berthierine (Longstaffe unpublished data).

Structural formulae were calculated for the samples using the procedure described by Brindley (1982). Since berthierine belongs to the serpentine group, it can be represented by the formula $(\text{R}^{2+}_a\text{R}^{3+}_b\Box_c)(\text{Si}_{2-x}\text{Al}_x)\text{O}_5(\text{OH})_4$ where R^{2+} and R^{3+} are cations occupying octahedral positions, \Box represents possible vacant octahedral positions, and $a + b + c = 3$ (Brindley 1982). To calculate its structural formula, the total valence of cations in tetrahedral and octahedral positions was normalized to +14. Measurements of H_2O^+ and H_2O^- were not used in the calculation since the procedure corresponds to an ideal oxygen and water content of $\text{O}_5(\text{OH})_4$. Using the ideal calculation, all samples with the exception of 1-7, showed an excess of water. The specimen with the highest content of 1.4 nm impurity (3-45) had the largest H_2O excess. Oxides of cations unable to enter octahedral sites (e.g., Na, Ca and K) are included in the table of chemical analysis for completeness but were not used in the structural formulae

calculations. These impurities likely result from trace quantities of illite and feldspar not detectable by XRD (even using a rotating anode system). Traces of Fe-rich smectitic clays may be responsible for some of the calcium. The effect of mineralogical impurities on the number of vacancies calculated for berthierine is limited at the levels present in these highly purified samples. For example, a change of 1 wt% SiO_2 resulting from an impurity produces a change of 0.017 in the calculated number of octahedral vacancies. Hence, relatively large quantities of impurities, easily detectable by rotating anode XRD, would be necessary to substantially skew the calculated result. The elements Ti, Ni and Zn, which are known to enter the berthierine structure (e.g., Arima et al. 1985; Bailey 1988b), also have not been included in the structural formulae calculations. They were omitted to facilitate direct comparison with other reported berthierine compositions. When titanium is included in structural formulae, there is a slight increase in the quantity of aluminum in the tetrahedral sheet. Titanium's tetravalent charge results in an even greater number of calculated vacancies (0.020 to 0.052) in the octahedral sheet.

Table 3 lists Mössbauer parameters for the five Clearwater berthierines, using a three doublet fit model, and compares these results with other berthierines. $\text{Fe}^{2+}/\text{Fe}^{3+}$ ratios were obtained using the relative areas of Fe^{2+} and Fe^{3+} absorptions. No corrections were made for possible differences in recoil-free fractions between Fe^{2+} and Fe^{3+} . For all samples, data from the two sides of the mirror-imaged spectra were folded and analyzed together. The spectra were fit with Lorentzian lines by a least-squares procedure with two different models (two doublets versus three doublets). In both models, the peaks of a given doublet were constrained to have equal areas and half-widths.

In the first model, one doublet was fitted for each of Fe^{2+} and Fe^{3+} . This gave quadrupole splittings ranging from 2.57 to 2.61 mm/s^{-1} and isomer shifts from 1.01 to 1.03 mm/s^{-1} for the ferrous doublet, and 0.71 to 0.95 mm/s^{-1} for the quadrupole splitting and 0.18 to 0.30 mm/s^{-1} for the isomer shifts for the ferric doublet. Chi^2 values ranged between 2.49 and 8.43. These values are similar to those of Coey et al. (1981) and Mackenzie and Berzowski (1984) where two doublet fits were also used. The second model, in which a three doublet fit was employed, achieved a closer approximation of the distribution of quadrupole splittings of Fe^{2+} by fitting two doublets to the Fe^{2+} resonant absorption (Figure 9). This resulted in a significant decrease in Chi^2 values; these data are given in Table 3. The quantity of Fe^{2+} and Fe^{3+} determined from peak areas was essentially identical regardless of which model was used. A four-doublet fit was attempted but required physically implausible peak widths.

The presence of non-equivalent ferrous and ferric octahedral sites in berthierine has been reported pre-

Table 3. Mössbauer data for Clearwater and other reported berthierines.

Sample	Chi-squared		QS ¹	IS ²	Width	Area
1-7	1.32	Fe ²⁺ (I) ³	2.37	1.11	0.311	0.273
		Fe ²⁺ (II) ³	2.69	1.13	0.284	0.508
		Fe ³⁺	0.69	0.41	0.540	0.219
1-16	1.54	Fe ²⁺ (I)	2.43	1.11	0.334	0.517
		Fe ²⁺ (II)	2.72	1.12	0.262	0.297
		Fe ³⁺	0.77	0.39	0.537	0.186
2-24	2.00	Fe ²⁺ (I)	2.34	1.11	0.293	0.216
		Fe ²⁺ (II)	2.68	1.12	0.293	0.544
		Fe ³⁺	0.74	0.41	0.537	0.241
2-29	1.62	Fe ²⁺ (I)	2.33	1.11	0.307	0.186
		Fe ²⁺ (II)	2.66	1.12	0.307	0.565
		Fe ³⁺	0.74	0.41	0.526	0.249
3-45	1.56	Fe ²⁺ (I)	2.36	1.12	0.307	0.243
		Fe ²⁺ (II)	2.69	1.13	0.287	0.559
		Fe ³⁺	0.74	0.41	0.482	0.199
Norway berthierine ⁴		Fe ²⁺	2.25	1.22		
		Fe ³⁺ (I)	1.11	0.33		
		Fe ³⁺ (II)	0.76	0.26		
Japan berthierine ⁴		Fe ²⁺	2.58	1.13		
		Fe ³⁺	1.09	0.25		
France berthierine ⁵		Fe ²⁺	2.57	1.13		
		Fe ³⁺	0.78	0.38		
USSR berthierine ⁶		Fe ²⁺ (I)	2.78	1.13		
		Fe ²⁺ (II)	2.43	1.16		
		Fe ³⁺	0.97	0.21		

¹ QS = quadrupole splitting (mm/sec).

² IS = isomer shift (mm/sec) relative to iron metal with $g_0 = 3.9156$ mm/s and $g_1 = 2.2363$ mm/s (Stevens and Stevens 1972).

³ (I) and (II) represent non-equivalent sites.

⁴ Mackenzie & Berezowski (1984).

⁵ Coey et al. (1981).

⁶ Yerzhova et al. (1975).

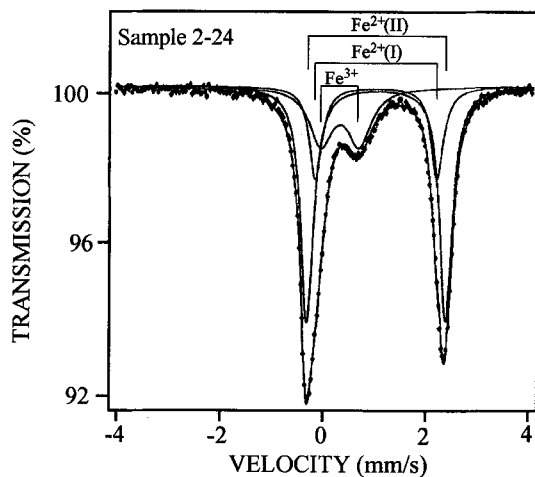


Figure 9. Mössbauer spectrum for sample 2-24 showing a three doublet fit.

viously (Yerzhova et al. 1976, 1982; Mackenzie and Berezowski 1984). Non-equivalent Fe²⁺-octahedral sites likely exist because the octahedral sheet is not saturated with Fe²⁺ (Coey et al. 1981). Substitution of trivalent (and possibly tetravalent) cations into the octahedral sheet causes distortion in both the size and symmetry of octahedral sites. The data for Clearwater berthierine support the suggestion that an increase in vacant octahedral sites resulting from R³⁺ (or R⁴⁺) substitution can cause an increase in the number of non-equivalent octahedral Fe²⁺ sites.

Broad ferric resonance absorptions suggest that Fe³⁺ also may be present in both octahedral sites (Bancroft 1973). Similarly, Bailey (1988c) reports asymmetry in the ferric doublet of a Mössbauer spectrum for an odinite sample from Senegal and suggests that odinite might also have non-equivalent Fe³⁺ sites. Substitution of Fe²⁺ and Mg²⁺ into a predominantly dioctahedral sheet likely causes similar structural distortion.

The chemical composition of the Clearwater berthierine is illustrated in Figure 10 using similar ternary diagrams to those presented earlier by Odin (1988) and

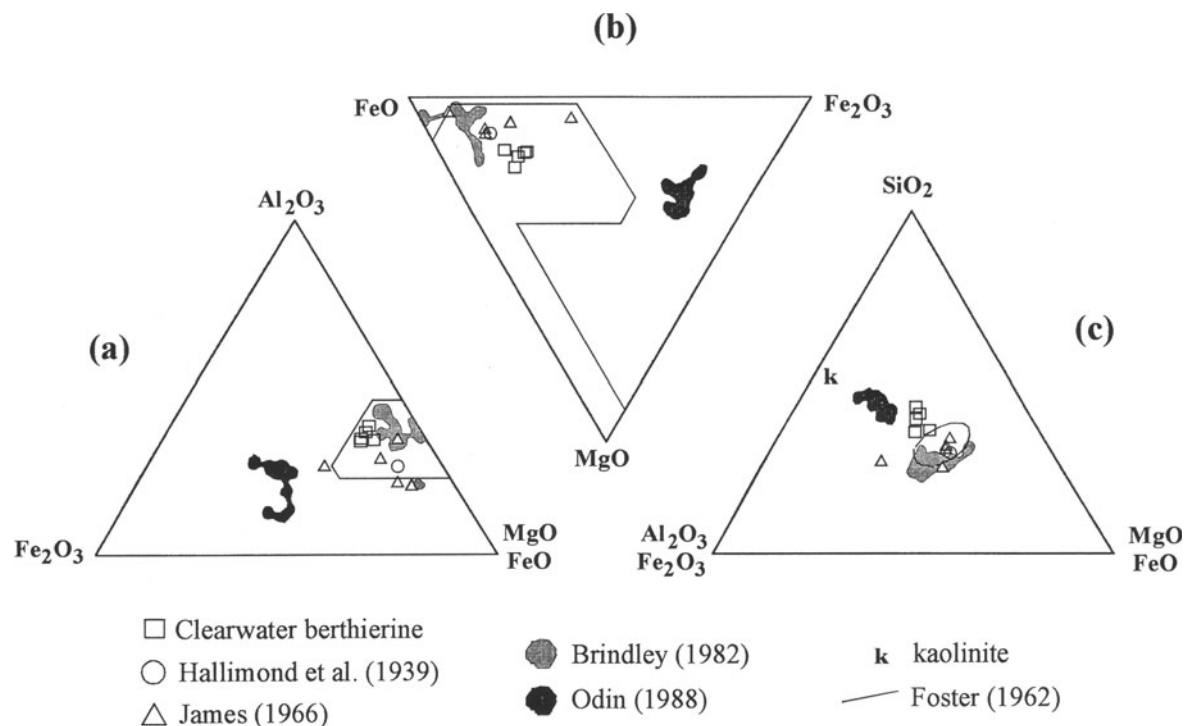


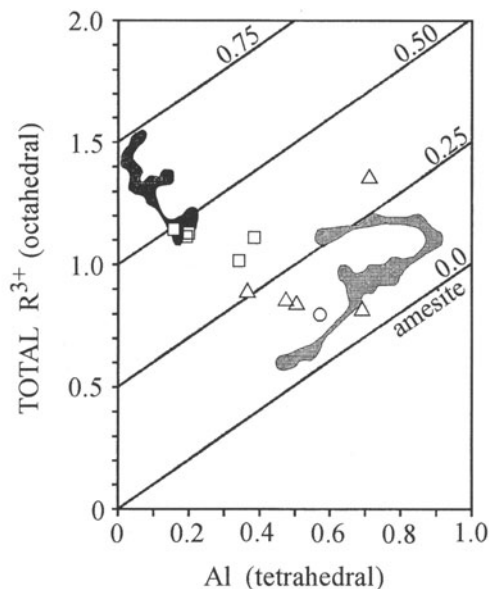
Figure 10. Ternary diagrams illustrating the chemical composition of Clearwater berthierine relative to other berthierines and odinite (Odin 1988). The thin lines enclose the range of compositions reported by Foster (1962) for 154 samples of chlorite. Figure 10c also illustrates the composition of kaolinite (k).

Bailey (1988b,c). The five Clearwater berthierine samples are plotted along with specimens from Hallimond et al. (1939), James (1966) and Brindley (1982). The compositions of odinite (Odin 1988) and chlorite (Foster 1962) are also indicated. Clearwater berthierines have a total divalent cation composition that is similar to other berthierines and which lies within the rather small chlorite field (Figure 10a). Clearwater berthierine's enrichment in Fe_2O_3 becomes more apparent when FeO and MgO are plotted separately (Figure 10b). The Clearwater samples are shifted toward the odinite field because of their higher MgO and Fe_2O_3 contents, but still lie well within the range of chlorite compositions reported by Foster (1962). Figure 10c best expresses the unique aspects of Clearwater berthierine chemistry, particularly their position between fully dioctahedral and dominantly trioctahedral structures. The Fe^{3+} -rich odinites plot nearest to the kaolinite field, whereas the majority of berthierines previously reported in the literature plot farthest away. Clearwater berthierine with its high SiO_2 and total R^{3+} contents lies between the previously reported data for odinite and berthierine.

In almost all berthierines reported to date, the number of R^{3+} cations in the octahedral sheet exceeds tetrahedral Al^{3+} , and electrical neutrality of layers is achieved by vacant octahedral sites (e.g., Brindley

1982). It has been suggested that siliceous impurities could cause apparent octahedral vacancies in both trioctahedral chlorites and berthierine (Jiang et al. 1992). Although mineralogical homogeneity can be verified by TEM, thus assuring AEM analyses are representative, analytical limitations prevent the determination of Fe^{2+}/Fe^{3+} at the same resolution. The assumption of layer charge neutrality and zero octahedral vacancies must then be employed to calculate iron valence states. While it is certain that siliceous impurities will affect the number of octahedral vacancies, the literature seems to support the existence of intermediate dioctahedral-trioctahedral 1:1 layer silicates (e.g., Bailey 1980; Brindley 1982).

Brindley (1982) found that when R^{3+} octahedral cations were plotted against tetrahedral Al^{3+} , most berthierine samples lay along a line with a slope of 1.3. A similar plot is shown in Figure 11, but also includes data from this study plus two other reports of berthierine and one of odinite. Structural formulae for odinite originally were calculated by Odin (1988) based on a chlorite structure. They have been recalculated here using the same method described for berthierine to permit a comparison among 1:1-layer structures. Diagonal lines on Figure 11 give the number of vacancies in the octahedral sheet with 0 corresponding to an ideal amesite (fully trioctahedral) and 1.0 a completely



- Clearwater Berthierine ● Odin (1988)
 ○ Hallimond et al. (1939) ● Brindley (1982)
 △ James (1966)

Figure 11. Trivalent octahedral cations versus tetrahedral aluminum for Clearwater berthierine, other berthierines (Hallimond et al. 1939; James 1966; Brindley 1982), and odinite (Odin 1988). The 0.0 line represent an octahedral sheet with no vacancies (ideally an amesite structure). The remaining lines (0.25, 0.50 and 0.75) represent the number of vacancies for a structure with 3 octahedral cation positions. The data of Odin (1988) were recalculated for a 1:1 layer structure based on the method of Brindley (1982).

dioctahedral mineral (e.g., kaolinite). The addition of data from Hallimond et al. (1939) and James (1966) significantly increase the amount of scatter in the berthierine data. Nevertheless, the majority of the data lie between 0 and 0.25 vacancies, except for Clearwater berthierine. Clearwater berthierine is enriched in Si and Fe³⁺ relative to most other reported berthierines. Although their Al content is low, the high Si content causes a greater proportion of the Al to reside in the octahedral sheet. The overall effect is to create a greater number of vacancies in the octahedral sheet, producing in this case a di-trioctahedral 1:1-layer mineral. Three of the samples plot within the lower range of odinite; the remaining two lie between odinite and other reported berthierines. Our data suggest that a range of dioctahedral-trioctahedral, iron-rich 1:1-layer silicates are present in the Clearwater Formation, with the concentrations of Si, Al and the proportion of ferric to ferrous iron determining the number of vacancies. Ideal odinite and berthierine may represent "end members" in such a series.

Table 4. $\delta^{18}\text{O}$ and δD -values for Clearwater berthierine.

Sample	$\delta^{18}\text{O}_{\text{V-SMOW}} \text{‰}$ Pretreatment Temperature			$\delta\text{D}_{\text{V-SMOW}}$
	110°C	150°C	300°C	
1-7		+11.43		-119.3
1-16		+11.22		-118.6
2-24	+9.95	+10.03	+10.86	-116.5
2-29		+10.84	+11.46	-122.4
3-45		+6.64		-118.6

Stable Isotope Analyses

Stepwise heatings under vacuum were performed to establish the pretreatment temperatures needed for stable isotope analysis, such that adsorbed water would be released but dehydroxylation would not begin prior to extraction of oxygen by fluorination methods. The first minor decrease in basal diffraction intensity was observed after heating at 150°C for 2 h. Slightly larger decreases were observed at 200 and 250°C with the first significant dehydroxylation occurring at about 300°C.

The variations in oxygen-isotope composition that accompanied pretreatment under vacuum for 2 to 3 h at 110°C, 150°C and 300°C are summarized in Table 4. Results at 110°C versus 150°C lie within experimental error of the method ($\pm 0.2\text{‰}$), but pretreatment at 300°C resulted in an increase in measured $\delta^{18}\text{O}$ values, probably because of incipient loss of low- ^{18}O hydroxyl groups. Accordingly, 150°C was selected as the optimum pretreatment temperature for oxygen-isotope analysis, similar to that used for other 1:1 layer silicates.

A berthierine-water, oxygen-isotope geothermometer was calculated using the average of the chemical compositions for Clearwater berthierine reported in Table 2 and the method of Savin and Lee (1988):

$$1000 \ln \alpha = 5.174(10^3)T^{-1} + 2.483(10^6)T^{-2} - 0.430(10^9)T^{-3} + 0.039(10^{12})T^{-4} - 13.59 \quad [1]$$

where temperature (T) is given in °Kelvin. This equation differs from that reported by Longstaffe et al. (1992), primarily because the quantity of Si present in the tetrahedral sheet exceeds that assumed in the earlier calculation. Solutions to this equation, using the upper, lower and average values of $\delta^{18}\text{O}$ obtained for Clearwater berthierine are shown in Figure 12.

Figure 12 shows that for reasonable temperatures of berthierine crystallization (25–45°C) in the early diagenetic environment, the $\delta^{18}\text{O}$ value of water ranged from about -14 to -6‰, averaging -10 to -8‰ (V-SMOW). Such values are typical of brackish to fresh water, rather than "normal" seawater ($\delta^{18}\text{O} \sim 0\text{‰}$). Even if all berthierine crystallized at maximum burial temperatures (about 60°C), the required porewater $\delta^{18}\text{O}$ values were substantially less than 0‰. Perhaps

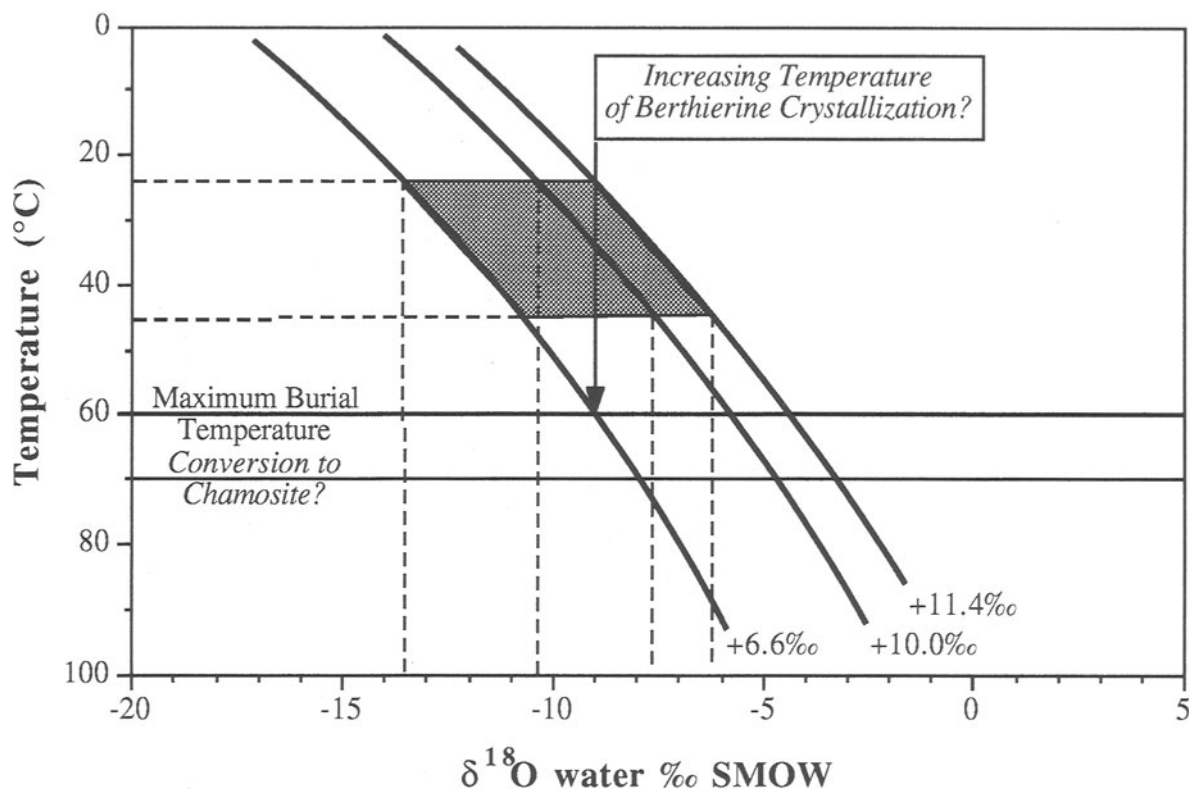


Figure 12. Temperature versus $\delta^{18}\text{O}$ value of porewater during crystallization of berthierine. The thick curves have been calculated for the lowest (+6.6‰), average (+10.0‰) and highest (+11.4‰) $\delta^{18}\text{O}$ values obtained for berthierine (see text). The solid horizontal lines indicate the maximum burial temperature for the Clearwater Formation, and the suggested minimum temperature for conversion of berthierine to chamosite. The shaded area indicates the range of porewater oxygen isotopic composition for berthierine crystallization between 25 and 45°C (likely interval of most intense crystallization). Crystallization from -9‰ water (i.e., brackish or meteoric) as temperatures rose from +25 to +60°C (arrow) can explain the entire range of berthierine $\delta^{18}\text{O}$ values.

notably, the sample with the lowest $\delta^{18}\text{O}$ value (3-45, Table 4) also contains the highest fraction of inseparable "chamosite" material. If this particular clay formed at the maximum burial temperature (about 60°C), a porewater with $\delta^{18}\text{O} = -9\text{‰}$ would be required, virtually identical to the average value predicted for the crystallization of more ^{18}O -rich, pure berthierine samples at lower temperatures. Similar porewater $\delta^{18}\text{O}$ values were reported by Longstaffe et al. (1992) for formation of the earliest diagenetic calcite in the berthierine-bearing sands.

The small range of δD values obtained for the Clearwater berthierines (-122 to -116‰ , Table 4) lacks unequivocal explanation, but nevertheless points to an important role for meteoric water in berthierine development. Meteoric porewaters with $\delta^{18}\text{O}$ values of -10 to -8‰ should have δD values of about -70 to -50‰ , according to the relationship of Craig (1961). At shallow diagenetic temperatures (e.g., $\leq 60^\circ\text{C}$), the Fe-chlorite-water permil fractionation for hydrogen is about $-40 \pm 5\text{‰}$ (Marumo and Longstaffe unpublished data). Assuming that berthierine behaves similarly, δD

values of $-100 \pm 10\text{‰}$ can be predicted for the clay. The measured δD values are lower, perhaps indicating a poor understanding of the hydrogen-isotope fractionation between Fe^{3+} -bearing berthierine and water. Alternatively, the δD values of the porewaters may have been lower than predicted using the meteoric water line; such behavior is characteristic of many formation waters (Longstaffe 1989). It is also possible that hydrogen with very low δD values was contributed to berthierine during microbial fermentation processes (Longstaffe et al. 1992). We also cannot rule out the possibility that berthierine preferentially exchanged hydrogen isotopes with meteoric water prior to emplacement of hydrocarbons or during hydrocarbon degradation. In other Cretaceous sandstones from the western Canada sedimentary basin, Longstaffe and Ayalon (1990) showed that hydrogen-isotope exchange occurred between kaolinite and meteoric water to temperatures as low as 40°C, without any corresponding change in the original oxygen-isotope composition of the clay. This exchange produced clay δD

values that are very similar to those obtained here for berthierine.

Berthierine Genesis

Primary crystallization of berthierine requires a supply of iron and reducing conditions (Curtis and Spears 1968; Curtis 1985). The classification of Berner (1981) further describes this environment to be sulfide and organic matter-poor, and anoxic; however, it must be marginally more oxic (post-oxic) than the environment in which siderite precipitates. The sediments must contain enough organic matter such that all dissolved oxygen may be consumed by aerobic microorganisms, and decomposition may then follow successively by nitrate, manganese and iron-reducing bacteria. Waters with low sulfate concentrations, brackish or freshwaters, are strongly favored since activity by sulfate-reducers is greatly restricted. The lack of O_2 and H_2S permits Fe^{2+} to accumulate to saturation. Because of low solubility, iron silicate(s) then can precipitate rapidly, relative to iron carbonate.

Berthierine's mode of occurrence and relationship to other minerals in the Clearwater Formation sands suggest that it formed early in diagenesis. Its oxygen isotopic compositions indicate that berthierine crystallization involved early porewaters that contained a sizeable fraction of meteoric water. The deltaic or estuarine setting proposed for the Clearwater sands can account in a general way for the dominance of brackish to fresh porewaters throughout diagenesis, as inferred from the oxygen-isotope compositions of all diagenetic minerals (Longstaffe 1993).

The low content of co-existing pyrite in the berthierine-rich portions of the Clearwater Formation, and hence the inferred low concentration of sulfate, also are consistent with brackish or fresh early porewaters, and/or low concentrations of organic matter during early diagenesis. Relatively low organic carbon contents are not unreasonable in such a setting. Typical carbon accumulation rates in coastal settings commonly range from 0.2 to 5 g C m⁻² y⁻¹ (Nedwell 1984, cf. freshwater lakes <30 to 160 g C m⁻² y⁻¹).

High sedimentation rates in a deltaic/estuarine setting would trap porewaters under conditions that quickly became anoxic. In addition, the large supply of readily dissolvable volcanic rock fragments represent an abundant supply of Fe. Under such conditions, berthierine and related Fe-rich clays may have crystallized directly from solutions that were saturated in iron, especially Fe^{2+} , but poor in bicarbonate. In localities rich in berthierine, only sporadic occurrences of early diagenetic siderite are observed. It seems that the methanic conditions conducive to carbonate (siderite, in particular) formation (e.g., Berner 1981) did not exist while dissolved Fe^{2+} was abundant.

Fe derived from dissolution of volcanic rock fragments also may have accumulated initially as "Fe-ooz-

es" accreted about sand grains by moving currents in a distributary channel-type environment (Longstaffe et al. 1992). Berthierine subsequently formed when these oxides and hydroxides were remobilized as reducing conditions were established.

Because of the deficiency in sulfate, reflecting dominantly fresh porewaters, a rather direct transition from post-oxic to methanic conditions probably occurred in the Clearwater sands. The appearance of ¹³C-rich (up to +23‰, Longstaffe 1994) calcite (rather than siderite) after berthierine in these sands suggests that most iron had been removed from the porewaters into berthierine and related clays by the time that methanogenic processes became dominant.

High $\delta^{13}C$ values (e.g., >+10‰) for carbon dioxide associated with microbial methane production are not all that common in most diagenetic settings. Lower values are generally the product of fermentation (Clayton pers. comm. 1992). Only under conditions of extensive CO₂ reduction, during which much of the ¹²C-rich carbon dioxide is preferentially consumed by microbes, will ¹³C-rich, residual carbon dioxide become available for carbonate precipitation. In the case of the Clearwater sands, it may be that the microbial population in the absence of sulfate, but in the presence of organic matter, acted first to reduce Fe^{3+} to Fe^{2+} , hence triggering berthierine crystallization in the post-oxic zone. Once Fe^{3+} was depleted and Fe in general fixed into clays, the microbes then began to reduce CO₂, leading to crystallization of the extremely ¹³C-rich calcite (Longstaffe 1994). Later emplacement of hydrocarbons has preserved both the berthierine and high $\delta^{13}C$ calcite from subsequent substantial diagenetic modification.

Possible Relationships with Odinite and other Fe-rich Clay Minerals

While the above model presents a plausible case for primary crystallization of berthierine, its peculiar composition in the Clearwater Formation prompts consideration of additional formation mechanisms. For example, in ironstones at least, Odin (1988) has suggested that poorly crystallized, syn-sedimentary marine clays with a serpentine structure (e.g., odinite) can recrystallize to form berthierine and chamosite during diagenesis in the absence of open contact with seawater. Modern occurrences of odinite peloids are restricted to tropical and subtropical locations. They typically form in estuarine environments under fluvial influence (Odin and L  tolle 1980). Porrenga (1967) reported that odinite crystallized at shallow depths at temperatures between 25 and 27°C, whereas lower temperatures favored glauconite formation. In these respects, berthierine in the Clearwater Formation sands fits the observation that most odinite occurrences are reported near river mouths. Furthermore, warm surface temperatures characteristic of odinite

formation probably were typical during the early Cretaceous deposition of the Clearwater Formation sands.

The chemical data obtained for Clearwater berthierine suggest that it is a compositional intermediate between most reported odinite and berthierine. For example, Clearwater berthierine is enriched in Fe^{3+} and Si relative to most berthierines, but depleted of these elements relative to odinite. Likewise, Al contents lie between reported maxima for odinite and minima for berthierine. In addition, while Clearwater berthierine appears to be well-crystallized relative to odinite, it nevertheless contains a considerably higher proportion of vacancies in the octahedral sheet than other berthierines reported in the literature. Accordingly, we propose that a spectrum of diagenetic, Fe-rich serpentine minerals can occur between the end-member compositions currently known for "ideal" berthierine and odinite.

The valence state of Fe commonly provides one of the critical distinguishing features between berthierine and odinite. However, the experimental ease of post-crystallization transformation between ferrous and ferric forms of berthierine during heating is well known (Brindley and Youell 1953; Mackenzie and Berezowski 1985). The depositional setting of the Clearwater sands affords at least two special opportunities for conversion of Fe^{3+} to Fe^{2+} in the Fe-serpentine. First, in this fresh to brackish environment, Fe-reducing microbes may have filled the biological niche normally occupied by sulfate reducers in more marine settings. That special energetic strategies were required by the microbial population during early diagenesis of the berthierine-rich sands has been demonstrated already by crystallization of ^{13}C -rich calcite shortly following berthierine crystallization. The very high values reflect the composition of residual CO_2 that survived large-scale microbial reduction of the CO_2 itself (Longstaffe 1993, 1994). Hence, the possibility of direct, microbial Fe-reduction of pre-existing, Fe-rich clays should not be dismissed.

A second and even more intriguing possibility, is that the emplacement of hydrocarbons, which probably was important in preservation of Clearwater berthierine, also created intense reducing conditions. In such an environment, intra-structural iron reduction could occur, and depending on its rate, one might expect an increase of the $\text{Fe}^{2+}/\text{Fe}^{3+}$ ratio in the Fe-serpentine over time.

The structural and chemical comparison between berthierine and odinite, and Clearwater berthierine's central position between them, is evident. However, the pore-lining or grain-coating character of Clearwater berthierine is not at all similar to the morphology generally associated with odinite. In Recent sediments, odinite is almost always reported as infillings resulting from impregnation or replacement of biogenic or detrital porous grains (e.g., Bailey 1988c; Odin

1988). The absence of such odinite in ancient sediments probably reflects its instability under reducing conditions on geological time scales. Reactions involving this poorly crystalline, Fe^{3+} -rich phase undoubtedly have contributed to formation of more stable, Fe-bearing phases, including Fe-clay minerals.

We predict however, that examples of pore-lining or grain-coating odinite-berthierine intermediates, like the Clearwater example described here, are more common in the Recent sediment record and simply await recognition and description. It seems likely that the structure and chemistry of these neoformed Fe-rich clays would evolve with burial and time toward phases with higher crystallinity and $\text{Fe}^{2+}/\text{Fe}^{3+}$ ratios, the latter because of intra-structural Fe-reduction. Because such modifications should involve only limited breaking of bonds involving oxygen, $\delta^{18}\text{O}$ values characteristic of primary crystallization conditions are likely to be preserved within the Fe-serpentine group minerals.

Such comments open the way to consideration of possible relationships among the 0.7 nm odinite-berthierine "series," chamosite and Fe-rich smectitic clays. Both of the latter phases are present in the Clearwater sands, the first in relatively small quantities together with berthierine and the second in ever increasing abundance, in more "marine" portions of the deltaic/estuarine system where berthierine contents dramatically decrease (Longstaffe et al. 1992; Longstaffe 1993, 1994). Further discussion of chamosite is rendered impossible at present by the difficulty in separating a pure sample from co-existing berthierine. However, we emphasize that Clearwater berthierine samples containing the least chamosite (and Fe-rich smectite) have the highest crystallinity. Separates with higher chamosite and Fe-smectite contents have characteristic diffractions for berthierine that are broader and of lower intensity. At least for berthierine and chamosite, we may be witnessing the incipient, low temperature (about 60°C) stages of a 0.7 nm to 1.4 nm transformation. Speculation on possible structural (and genetic) relationships between Clearwater berthierine and associated, Fe-rich smectitic clays must be deferred, pending completion of detailed structural and chemical investigations of the swelling clay (Longstaffe in progress).

As a final note, we return to the observation that Fe-rich chlorite (chamosite) is abundant as grain-coatings and early pore linings in many ancient sandstones. These chloritic rims, where they are not too thick, are well known to preserve porosity and permeability of potential hydrocarbon reservoir rocks by inhibiting further growth of diagenetic minerals. In contrast, development of very thick rims of Fe-rich chlorite has been shown to reduce hydrocarbon saturation, and increase the potential for formation damage during secondary and tertiary hydrocarbon recovery (Longstaffe 1990). Almost always, sandstones contain-

ing these Fe-chlorite rims have experienced burial temperatures exceeding 70°C. The origin of the Fe-chlorite rim has remained speculative, particularly whether it had a precursor, what that might have been, and what depositional environments and early diagenetic porewaters favored its development (e.g., Longstaffe 1986; Ayalon and Longstaffe 1988). Hillier (1994) has suggested that berthierine (and possibly odinite) may be low temperature precursors to chamosite. A smectitic precursor is favored by Hillier (1994) for Mg-chlorites, although Humphreys et al. (1994) report an Fe-rich chlorite that possibly was derived from smectite. We believe that the Clearwater Formation and the diagenetic berthierine that it contains, provide a useful illustration of the environmental and chemical conditions that can initiate Fe-chlorite rim development, and answer at least some mineralogical questions about the nature of early Fe-chlorite precursors in many sandstones.

CONCLUSIONS

Networks of laths of well-crystallized berthierine form pore-linings or grain-coatings of variable thickness on framework grains in the Cretaceous Clearwater Formation oil-sands of northeastern Alberta, Canada. The berthierine is a primary precipitate that crystallized early in diagenesis within portions of a deltaic/estuarine complex dominated by fresh to brackish water. Both monoclinic and ortho-hexagonal forms of berthierine are present in approximately equal proportions. Minor amounts of chamosite, and variable quantities of Fe-smectitic clays, also occur together with the berthierine.

The Clearwater Formation berthierine has a chemical composition intermediate between most reported odinites and berthierines. These results suggest that a series of compositions between ideal Fe-serpentine "end-members" is possible. The large number of vacancies in the Clearwater Formation berthierine suggest that it has a di-trioctahedral structure. Berthierine has been preserved in abundance in this particular setting because temperatures during diagenesis did not exceed 70°C, and also because emplacement of hydrocarbons (now degraded to heavy oil) early in the diagenetic history attenuated subsequent transformation of berthierine to other phases, such as chamosite. Post-crystallization, intra-structural reduction of Fe³⁺ to Fe²⁺ in the berthierine may have occurred during intense microbial activity and/or because of the strongly reducing environment created by emplacement of hydrocarbons. This rather special example of Fe-clays provides valuable insights into the relationship between the Fe-serpentine minerals, odinite and berthierine, and points rather directly to their importance as precursors to early diagenetic, grain-coating and pore-lining Fe-chlorite (chamosite) in ancient deltaic/estuarine sandstones.

ACKNOWLEDGMENTS

Funding was provided by the Natural Sciences and Engineering Research Council of Canada (Research grant #A7837 to FJL) and AOSTRA University-Industry Contract #680. Paul Middlestead is thanked for capable assistance with the isotope measurements. Bob Barnett provided help in the electron microprobe laboratory. We thank Bob Luth (Department of Geology, University of Alberta) for performing the Mössbauer analyses, Ron Maslen (Department of Chemistry, University of Western Ontario) for access to the infrared spectrometer and Surface Science Western for access to the scanning electron microscope. We thank S. Hillier and an anonymous reviewer for their helpful comments on an earlier version of this paper. We are grateful for the editorial assistance of R. Ferrell and W.H. Hudnall.

REFERENCES

- Ahn JH, Peacor DR. 1985. Transmission electron microscopic study of diagenetic chlorite in Gulf Coast argillaceous sediments. *Clays & Clay Miner* 33:228–236.
- Amouric M, Gianetto I, Proust D. 1988. 7, 10, and 14 Å mixed-layer phyllosilicates studied structurally by TEM in pelitic rocks of the Piemontese zone (Venezuela). *Bull Mineral* 111:29–37.
- Arima M, Fleet MA, Barnett RL. 1985. Titanian berthierine: A Ti-rich serpentine-group mineral from the Picton ultramafic dyke, Ontario. *Can Mineral* 23:213–220.
- Ayalon A, Longstaffe FJ. 1988. Oxygen isotope studies of diagenesis and pore-water evolution in the western Canada sedimentary basin: evidence from the Upper Cretaceous basal Belly River sandstone, Alberta. *J Sed Petrol* 58:489–505.
- Bailey SW. 1980. Structures of layer silicates. In: Brindley GW, Brown G, editors. *Crystal Structures of Clay Minerals and their X-ray Identification*. Washington: Mineralogical Society of America. p 2–123.
- Bailey SW. 1988a. Polytypism of 1:1 layer silicates. In: Bailey SW, editor. *Hydrous Phyllosilicates (exclusive of micas)*. Washington: Mineralogical Society of America. p 9–27.
- Bailey SW. 1988b. Structures and compositions of other trioctahedral 1:1 phyllosilicates. In: Bailey SW, editor. *Hydrous Phyllosilicates (exclusive of micas)*. Washington: Mineralogical Society of America. p 169–188.
- Bailey SW. 1988c. Odinite, a new dioctahedral-trioctahedral Fe³⁺-rich 1:1 clay mineral. *Clay Miner* 23:237–247.
- Bancroft GM. 1973. *Mössbauer Spectroscopy: An introduction for inorganic chemists and geochemists*. New York: John Wiley and Sons.
- Beaumont C, Boutilier R, Mackenzie AS, Rullkotter J. 1985. Isomerization and aromatization of hydrocarbons and the paleothermometry and burial history of the Alberta Foreland Basin. *Am Assoc Pet Geol Bull* 69:546–566.
- Berner RA. 1981. A new geochemical classification of sedimentary environments. *J Sed Petrol* 51:359–365.
- Bhattacharyya DP. 1983. Origin of berthierine in ironstones. *Clays & Clay Miner* 31:173–182.
- Bigeleisen J, Pearlman ML, Prosser HC. 1952. Conversion of hydrogenic materials to hydrogen for isotopic analysis. *Anal Chem* 24:1356–1357.
- Brindley GW. 1949. Mineralogy and crystal structure of chamosite. *Nature* 164:319–320.
- Brindley GW. 1951. The crystal structures of some chamosite minerals. *Mineral Mag* 29:502–525.
- Brindley GW. 1961. Kaolin, serpentine, and kindred minerals. In: Brown G, editor. *The X-Ray Identification and Crystal Structures of Clay Minerals*. London: Mineralogical Society (Clay Minerals Group). p 51–131.

- Brindley GW. 1981. Structures and chemical compositions of clay minerals. In: Longstaffe FJ, editor. *Short Course in Clays and the Resource Geologist* Calgary: Mineralogical Association of Canada. p 1–21.
- Brindley GW. 1982. Chemical compositions of berthierines—A review. *Clays & Clay Miner* 30:153–155.
- Brindley GW, Youell RF. 1953. Ferrous chamosite and ferric chamosite. *Mineral Mag* 30:57–70.
- Brindley GW, Bailey SW, Faust GT, Forman SA, Rich CI. 1968. Report of the Nomenclature Committee (1966–67) of the Clay Minerals Society. *Clays & Clay Miner* 16:322–324.
- Clayton C. 1992. School of Geological Sciences. Kingston University, Penrhyn Road, Kingston upon Thames, Surrey, United Kingdom KT1 2EE.
- Clayton RN, Mayeda TK. 1963. The use of bromine pentafluoride in the extraction of oxygen from oxides and silicates for isotopic analysis. *Geochim Cosmochim Acta* 27:43–52.
- Coey JMD, Ballet O, Moukarika A, Soubeyroux JL. 1981. Magnetic properties of sheet silicates: 1:1 layer minerals. *Phys Chem Miner* 7:141–148.
- Craig H. 1961. Isotopic variations in meteoric waters. *Science* 133:1702–1703.
- Curtis CD. 1985. Clay mineral precipitation and transformation during burial diagenesis. *Phil Trans Roy Soc Lond A315:91–105*.
- Curtis CD. 1990. The critical importance of diagenetic zones in determining sediment mineralogy. *Geol Assoc Can Prog Abstr* 15:A29.
- Curtis CD, Spears DA. 1968. The formation of sedimentary iron minerals. *Econ Geol* 24:257–270.
- Dean RS, Nahnybida C. 1985. Authigenic trioctahedral clay minerals coating Clearwater Formation sand grains in Cold Lake, Alberta—extended abstract. *Appl Clay Sci* 1:237–238.
- Farmer VC. 1974. The layer silicates. In: Farmer VC, editor. *The Infrared Spectra of Minerals*. Monograph 4. London: Mineralogical Society.
- Folk RL. 1974. *Petrology of Sedimentary Rocks*. Austin, Texas: Hemphill Publishing Company. 170p.
- Foster MD. 1962. Interpretation of the composition and a classification of the chlorites. *US Geol Surv Prof Pap* 414A:1–33.
- Hacquebard PA. 1977. Rank of coal as an index of organic metamorphism for oil and gas in Alberta. In: Deroo G, Powell T, Tissot B, McCrossan R, editors. *The Origin and Migration of Petroleum in the Western Canadian Sedimentary Basin*, Alberta Geol Surv Can Bull 262:11–22.
- Hallimond AF, Harvey CO, Bannister IA. 1939. On the relation of chamosite and daphnite to the chlorite group. *Mineral Mag* 25:441–465.
- Harrison DB, Glaister RP, Nelson HW. 1981. Reservoir description of the Clearwater oil sand Cold Lake, Alberta Canada. In: Meyer RF, Steele CT, editors. *Proc 1st Int Conf on the Future of Heavy Crude and Tar Sands*. New York: McGraw-Hill. p 264–279.
- Hillier S. 1994. Pore-lining chlorites in siliciclastic reservoir sandstones: electron microprobe, SEM and XRD data, and implications for their origin. *Clay Miner* 29:665–679.
- Hillier S, Velde B. 1992. Chlorite interstratified with a 7 Å mineral: an example from offshore Norway and possible implications for the interpretation of the composition of diagenetic chlorites. *Clay Miner* 27:475–486.
- Humphreys B, Smith SA, Strong GE. 1989. Authigenic chlorite in late Triassic sandstones from the Central Graben, North Sea. *Clay Miner* 24:427–444.
- Humphreys B, Kemp SJ, Lott GK, Bermanto, Dharmayanti DA, Samsori I. 1994. Origin of grain-coating chlorite by smectite transformation: An example from Miocene sandstones, North Sumatra back-arc basin, Indonesia. *Clay Miner* 29:681–692.
- Hutcheon I, Abercrombie H, Putnam P, Gardner R, Krouse R. 1989. Sedimentology and diagenesis of the Clearwater Formation at Tucker Lake. *Bull Can Pet Geol* 37:83–97.
- Iijima A, Matsumoto R. 1982. Berthierine and chamosite in coal measures of Japan. *Clays & Clay Miner* 30:264–274.
- Jahren JS, Aagaard P. 1989. Compositional variations in diagenetic chlorites and illites, and relationships with formation-water chemistry. *Clay Miner* 24:157–170.
- James HE. 1966. Chemistry of the iron-rich sedimentary rocks. *US Geol Surv Prof Pap* 440W:1–60.
- Jiang WT, Peacor DR, Slack JF. 1992. Microstructures, mixed layering, and polymorphism of chlorite and retrograde berthierine in the Kidd Creek Massive sulfide deposit, Ontario. *Clays & Clay Miner* 40:501–514.
- Kantorowicz JD, Bryant ID, Dawans JM. 1987. Controls on the geometry and distribution of carbonate cements in Jurassic sandstones: Bridport Sands, southern England and Viking Group, Troll Field, Norway. In: Marshall JD, editor. *Diagenesis of Sedimentary Sequences*. *Geol Soc Spec Publ* 36:103–118.
- Kodama H, Foscolos AE. 1981. Occurrence of berthierine in Canadian Arctic desert soils. *Can Mineral* 19:279–283.
- Kyser TK, O'Neil JR. 1984. Hydrogen isotope systematics of submarine basalts. *Geochim Cosmochim Acta* 48:2123–2133.
- Lee HH, Peacor DR. 1983. Interlayer transitions in phyllosilicates of Martinsburg shale. *Nature* 303:608–609.
- Longstaffe FJ. 1986. Oxygen isotope studies of diagenesis in the basal Belly River sandstone, Pembina I-Pool, Alberta. *J Sed Petrol* 56:78–88.
- Longstaffe FJ. 1989. Stable isotopes as tracers in clastic diagenesis. In: Hutcheon IE, editor. *Short Course in Burial Diagenesis*. Montreal: Mineralogical Association of Canada 15:201–277.
- Longstaffe FJ. 1990. An introduction to clastic diagenesis. In: Harrison WB III, editor. *Introduction to Diagenesis, Methods and Applications*. Ont Pet Inst Short Course. p 1–56.
- Longstaffe FJ. 1993. Meteoric water and sandstone diagenesis in the western Canada sedimentary basin. In: Horbury AD, Robinson AG, editors. *Diagenesis and Basin Development*. *Am Assoc Petrol Geol Study Geol* 36: p 49–68.
- Longstaffe FJ. 1994. Stable isotope constraints on sandstone diagenesis in the western Canada sedimentary basin. In: Parker A, Sellwood B, editors. *Quantitative Diagenesis: Recent Developments and Applications to Reservoir Geology*. NATO ASI Series: Kluwer Academic Publishers. p 223–274.
- Longstaffe FJ, Ayalon A. 1990. Hydrogen-isotope geochemistry of diagenetic clay minerals from Cretaceous sandstones, Alberta, Canada: evidence for exchange. *Appl Geochem* 5:657–668.
- Longstaffe FJ, Ayalon A, Racki M. 1989a. Natural diagenesis of Clearwater Formations reservoirs in the Cold Lake area, Alberta, Part I: Mineralogical studies. *Can Soc Pet Geol Annu Meet Prog Abstr*. p 130.
- Longstaffe FJ, Ayalon A, Racki M. 1989b. Natural diagenesis of Clearwater Formation reservoirs in the Cold Lake area, Alberta, Part II: Stable isotope studies of water/mineral interaction. *Can Soc Pet Geol Annu Meet Prog Abstr*. p 142.
- Longstaffe FJ, Racki MA, Ayalon A. 1992. Stable isotope studies of diagenesis in berthierine-bearing oil sands, Clearwater Formation, Alberta. In: Kharaka YK, Maest AS, editors. *Water Rock Interaction*. Vol.2: Moderate and High

- Temperature Environments, Proc 7th Int Symp on Water-Rock Interaction Rotterdam: AA Balkema. p 955–958.
- Longstaffe FJ, Tazaki K. Department of Earth Sciences, University of Western Ontario, London, Ontario, Canada N6A 5B7. Unpublished data.
- Marumo K, Longstaffe FJ. Department of Earth Sciences, University of Western Ontario, London, Ontario, Canada N6A 5B7. Unpublished data.
- MacKenzie KJD, Berezowski RM. 1984. Thermal and Mössbauer studies of iron-containing hydrous silicates. V. Berthierine. *Thermochim Acta* 74:291–312.
- Nedwell DB. 1984. The input and mineralization of organic carbon in anaerobic aquatic sediments. In: Marshall KC, editor. *Advanced Microbial Ecology* 7. New York: Plenum. p 93–132.
- Nikitina AP, Zvyagin BB. 1972. Origin and crystal structure features of clay minerals from the lateritic bauxites in the European part of the USSR. *Proc Int Clay Conf Madrid*. p 227–233.
- Odin GS, editor. 1988. *Green Marine Clays: Developments in Sedimentology* 45. Amsterdam: Elsevier.
- Odin GS, Giresse P. 1972. Formation de minéraux phylliteux (berthiérine, smectites, glauconite ouverte) dans les sédiments du Golfe de Guinée. *CR Acad Sci Paris* 274:177–180.
- Odin GS, Létolle R. 1980. Glauconitization and phosphatization environments: a tentative comparison. *Soc Econ Paleontol Mineral Spec Publ* 29:227–237.
- Odin GS, Matter A. 1981. De glauconiarum origine. *Sedimentol* 28:611–641.
- Porrenga DH. 1965. Chamosite in recent sediments of the Niger and Orinoco Deltas. *Geol Mijnbouw* 44:400–403.
- Porrenga DH. 1967. Glauconite and chamosite as depth indicators in the marine environment. *Mar Geol* 5:495–501.
- Prentice ME, Wightman DM. 1987. Mineralogy of the Clearwater Formation, Cold Lake oil sands: Implications for enhanced oil recovery. *Alberta Geol Surv Rep*. p 1–41.
- Putnam PE, Pedskalny MA. 1983. Provenance of Clearwater Formation reservoir sandstones, Cold Lake, Alberta, with comments on feldspar composition. *Bull Can Pet Geol* 31: 148–160.
- Rohrlich V, Price NB, Calvert SE. 1969. Chamosite in the recent sediments of Loch Etive, Scotland. *J Sed Petrol* 39: 624–631.
- Savin SM, Lee M. 1988. Isotopic studies of phyllosilicates. In: Bailey SW, editor. *Hydrous Phyllosilicates (exclusive of micas)*. Washington: Mineralogical Society of America. p 189–224.
- Schoen R. 1964. Clay minerals of the Silurian Clinton ironstones, New York State. *J Sed Petrol* 34:855–863.
- Serna CJ, Velde BD, White JL. 1977. Infrared evidence of order-disorder in amesites. *Am Min* 62:296–303.
- Siehl A, Thein J. 1989. Minette-type ironstones. In: Young TP, Taylor WEG, editors. *Phanerozoic Ironstones*. *Geol Soc Spec Publ* 46. p 175–193.
- Stevens IG, Stevens VE. 1972. *Mössbauer Effect Data Index, Covering the 1970 Literature*. IFI/Plenum Data Corporation.
- Taylor KG. 1990. Berthierine from the non-marine Wealden (Early Cretaceous) sediments of south-east England. *Clay Miner* 25:391–399.
- Tellier KE, Hluchy MM, Walker JR, Reynolds RC Jr. 1988. Application of high gradient magnetic separation (HGMS) to structural and compositional studies of clay mineral mixtures. *J Sed Petrol*: 761–763.
- Van Houten FB, Purucker ME. 1984. Glauconitic peloids and chamositic ooids—favorable factors, constraints, and problems. *Earth Sci Rev* 20(3):211–243.
- Velde B, Raoult JF, Leikine M. 1974. Metamorphosed berthierine pellets in Mid-Cretaceous rocks from northeastern Algeria. *J Sed Petrol* 44:1275–1280.
- Vennemann TW, O'Neil JR. 1993. A simple and inexpensive method of hydrogen isotope and water analyses of minerals and rocks based on zinc reagent. *Chem Geol (Isot Geosci Sect)* 103:227–234.
- Vigrass LW. 1968. Geology of Canadian heavy oil sands. *Amer Assoc Petr Geol Bull* 52:1984–1999.
- Visser K, Dankers PHM, Leckie D, Van Der Marel AGP. 1988. Mineralogy and geology of the Clearwater reservoir sands in the Wolf Lake Area, Cold Lake, Alberta. In: Meyer RF, editor. *Proc 3rd UNITAR/UNDP Int Conf on Heavy Crude and Tar Sands* New York: McGraw-Hill. p 119–133.
- Walker JR, Thompson GR. 1990. Structural variations in chlorite and illite in a diagenetic sequence from the Imperial Valley, California. *Clays Clay Miner* 38:315–321.
- Wightman DM, Berezniuk T. 1986. Resource characterization and depositional modelling of the Clearwater Formation, Cold Lake oil sands deposit, east-central Alberta. In: Westhoff JD, Marchant LC, editors. *Proc 1986 Tar Sands Symp Jackson, Wyoming: ARC Contribution No.1452*.
- Wightman DM, Rottenfusser B, Kramers J, Harrison R. 1989. Geology of the Alberta oil sands deposits. In: Heplet LG, Hsi C, editors. *AOSTRA Technical Handbook on Oil Sands, Bitumens and Heavy Oils*. AOSTRA Tech Publ Ser 6. p 1–9.
- Yershova ZP, Nikitina AP, Perfil'ev Yu D, Babeshkin AM. 1976. Study of chamosites by gamma-resonance (Mössbauer) spectroscopy. In: Bailey SW, editor. *Proc Int Clay Conf, Mexico City, 1975*. Wilmette, Illinois: Applied Publishing. p 211–219.
- Yershova KS, Kuzemkina Ye N, Dubakina LS, Solntseva LS, Tkacheva TV, Umnova Ye G, Shcherbak OV. 1982. Chamosite, a supergene iron-aluminum 7 Å-silicate. *Dokl Acad Sci USSR Earth Sci Sect* 265:123–125.
- Youell RF. 1955. Mineralogy and crystal structure of chamosite. *Nature* 176:560–561.
- Youell RF. 1958a. Isomorphous replacement in the kaolin group of minerals. *Nature* 181:557–558.
- Youell RF. 1958b. A clay mineralogical study of the ironstone at Easton Neston, Northamptonshire. *Clay Min Bull* 3:264–269.
- Zhou J. 1995. Alberta Research Council. Oil, Sand and Hydrocarbon Recovery. P.O. Box 8330 Station F, Edmonton, Alberta, Canada T6H 5X2.

(Received 30 November 1994; accepted 21 March 1995; Ms. 2598)